

Supporting Information

Multi-enzyme catalysed processes using purified and whole-cell biocatalysts towards a 1,3,4-substituted tetrahydroisoquinoline

Douglas Weber,^{a,b} Lucas de Souza Bastos,^a Margit Winkler,^{c,d} Yeke Ni,^e Abil E. Aliev,^e Helen C. Hailes^e and Doerte Rother^{a,b}

^aInstitute of Bio- and Geosciences (IBG-1): Biotechnology Forschungszentrum Juelich GmbH, 52425 Juelich, Germany.

^bAachen Biology and Biotechnology (ABbt), RWTH Aachen University, Worringer Weg 1, 52062 Aachen, Germany.

^cacib GmbH, Krenngasse 37, A-8010 Graz, Austria.

^dInstitute of Molecular Biotechnology, Graz University of Technology, Petersgasse 14, 8010 Graz, Austria.

^eDepartment of Chemistry, University College London, London, WC1H 0AJ, UK.

Table of content

1. Cultivation methods and protein purification	3
1.1. Host strains.....	3
1.2. CAR enzymes	3
1.3. Media and solutions for cultivations.....	4
1.4. Protein production	5
1.4.1. Pre-culture	5
1.4.2. Production of carboxylate reductases in 1L-shaking cultures.....	6
1.4.3. Production of whole-cell carboxylate reductases.....	6
1.4.4. Production of ATP-regenerating enzymes and the pyrophosphatase from <i>E. coli</i>	6
1.4.5. Production of the (<i>R</i>)-selective pyruvate decarboxylase variant	7
1.4.6. Production of transaminases	7
1.4.7. Production of the norcoclaurine synthase variant $\Delta Tf29NCS-A79I$	7
1.5. Protein purification	7
1.6. Determination of initial rates of CARs.....	11
2. Enzymatic production of compound standards.....	11
2.1. (1 <i>S</i> ,3 <i>S</i> ,4 <i>R</i>)-1-Benzyl-3-methyl-1,2,3,4-tetrahydroisoquinoline-4,6-diol	11
2.2. (1 <i>S</i> ,3 <i>S</i> ,4 <i>S</i>)-1-Benzyl-3-methyl-1,2,3,4-tetrahydroisoquinoline-4,6-diol	12
2.2.1. (<i>S</i>)-3-Hydroxyphenylacetylcarbinol	12
2.2.2. 3-((1 <i>S</i> ,2 <i>S</i>)-2-Amino-1-hydroxypropyl)phenol	13
2.2.3. (1 <i>S</i> ,3 <i>S</i> ,4 <i>S</i>)-1-Benzyl-3-methyl-1,2,3,4-tetrahydroisoquinoline-4,6-diol	13
2.3. NMR data	14
2.3.1. (1 <i>S</i> ,3 <i>S</i> ,4 <i>R</i>)-THIQ.....	14
2.3.2. (1 <i>S</i> ,3 <i>S</i> ,4 <i>S</i>)-THIQ	18
3. HPLC analytics.....	22
3.1. Method I.....	22
3.2. Method II.....	23

3.3. Method III.....	24
3.4. Method IV.....	25
4. Determination of process metrics	25
5. Supporting data	26
5.1. Substrate scope investigation of CAR enzymes.....	26
5.2. Conversion curves for 3-hydroxybenzoic acid.....	29
5.3. <i>In vitro</i> reduction of 3-hydroxybenzoic acid using long-term stored NoCAR	30
5.4. Determination of the stereoselectivity of the carboligase ApPDC-var.....	31
5.5. Cross-reactivity and possible formation of by-products in the cascade	32
5.6. Optimisation of the transamination reaction.....	33
5.6.1. Concentration of <i>BmTA</i>	33
5.6.2. Molar ratio of substrates	34
5.6.3. Reaction mode: closed/opened lid	35
5.6.4. Selection of enzyme and amine donor	36
5.6.5. Application of best reaction conditions in the cascade	37
5.7. Optimisation of the cyclisation reaction	38
5.7.1. Concentration of $\Delta 297fNCS-A79I$	39
5.7.2. Substrate molar ratio	40
5.7.3. Concentration of DMSO	41
5.8. Influence of varying amounts of CAR as lyophilised whole-cell catalysts in the reduction of 3-hydroxybenzoic acid.....	42
5.9. Increasing substrate loads in the bioreduction of 3-hydroxybenzoic acid catalysed by whole-cell catalysts.....	43
5.10. Proof-of-concept one-pot two-step cascade starting with renewable 3-OH-BZ.....	44
6. References	45

1. Cultivation methods and protein purification

1.1. Host strains

All host strains used in this work for the production of recombinant proteins are listed in Table S1.

Table S1. Overview of all host strains used in this work

Host	Strain	Key features
<i>Escherichia coli</i> (<i>E. coli</i>)	<i>E. coli</i> BL21(DE3)	It is a basic IPTG-inducible strain containing T7 RNAP (DE3). Genotype: <i>F- ompT lon hsdSB (rB-mB-) gal dcm</i> (DE3). ¹
	<i>E. coli</i> Tuner(DE3)	This strain contains mutated <i>lacZY</i> permease that allows for a more linear control of expression. Genotype: <i>F- ompT lon hsdSB (rB-mB-) gal dcm lacY1</i> (DE3). ^{1,2}
	<i>E. coli</i> K-12 MG1655 RARE(DE3)	This strain displays reduced endogenous reduction of aromatic and aliphatic aldehydes. Thus, the following genes were deleted from the <i>E. coli</i> K-12 MG1655 genome: <i>dkgB, yeaE, dkgA, yqhC, yqhD, yjgB, and yahK</i> . ³

1.2. CAR enzymes

Table S2. Specifications of the CAR enzymes used in this work

Enzyme	Abbreviation	Microorganism of origin	NCBI accession code	Reference
Carboxylate reductase (CAR)	<i>M</i> sCAR	<i>Mycobacterium smegmatis</i>	AFP42026.1	4
	<i>M</i> pCAR	<i>Mycobacterium phlei</i>	WP_003889896.1	4
	<i>N</i> bCAR	<i>Nocardia brasiliensis</i>	AFU02004.1	5
	<i>N</i> cCAR	<i>Neurospora crassa</i>	XP_955820.1	6
	<i>N</i> iCAR	<i>Nocardia iowensis</i>	WP_012393886	4,6
	<i>N</i> oCAR	<i>Nocardia otitidiscaviarum</i>	WP_029928026.1	4,7
	<i>T</i> pCAR	<i>Tsumakurella paurometabola</i>	WP_013126039.1	4
	<i>T</i> vCAR	<i>Trametes versicolor</i>	WP_013126039.1	8

1.3. Media and solutions for cultivations

Different media were used for the transformation, pre-culture and main culture. The composition of these media is shown in Table S3.

Table S3. Composition of media for cultivation

Medium/Solution	Abbreviation	Components	Final concentration
Super optimal broth	SOC	Glucose	20 mM
		KCl	2.5 mM
		MgCl ₂	10 mM
		NaCl	10 mM
		Peptone	20 g L ⁻¹
		Yeast extract	5 g L ⁻¹
Lysogeny broth	LB	NaCl	10 g L ⁻¹
		Peptone	10 g L ⁻¹
		Yeast extract	5 g L ⁻¹
Autoinduction	AI	Peptone	12 g L ⁻¹
		Yeast extract	24 g L ⁻¹
		Glycerol	5 g L ⁻¹
		Lactose monohydrate	2.2 g L ⁻¹
		Glucose monohydrate	0.52 g L ⁻¹
		KPi buffer	90 mM
Terrific broth	TB	Peptone	12 g L ⁻¹
		Yeast extract	24 g L ⁻¹
		Glycerol	5 g L ⁻¹
		10x KPi buffer	100 mL L ⁻¹
Potassium phosphate buffer	10x KPi (pH 7.0)	0.17 M KH ₂ PO ₄	23.1 g L ⁻¹
		0.72 M K ₂ HPO ₄	125.4 g L ⁻¹

Table S4 compiles the cultivation methods used to produce each enzyme used in this work.

Table S4. Overview of all enzymes produced in this work

Enzyme	Abbreviation	Source	Media used for cultivation
Transaminase	<i>BmTA</i>	<i>Bacillus megaterium</i>	AI
	<i>Cv2025</i>	<i>Chromobacterium violaceum</i>	AI
Carboxylate reductase	<i>MsCAR</i>	<i>Mycobacterium smegmatis</i>	TB
	<i>MpCAR</i>	<i>Mycobacterium phlei</i>	TB
	<i>NbCAR</i>	<i>Nocardia brasiliensis</i>	TB
	<i>NcCAR</i>	<i>Neurospora crassa</i>	TB
	<i>NiCAR</i>	<i>Nocardia iowensis</i>	TB
	<i>NoCAR</i>	<i>Nocardia otitidiscaviarum</i>	TB
	<i>TpCAR</i>	<i>Tsumakurella paurometabola</i>	TB
	<i>TvCAR</i>	<i>Trametes versicolor</i>	TB
Norcochlorine synthase	$\Delta 29TfNCS-A79I$	<i>Thalictrum flavum</i>	TB
Phosphate kinase	<i>MrPPK</i>	<i>Meiothermus ruber</i>	LB
	<i>SmPPK</i>	<i>Sinorhizobium meliloti</i>	LB
Pyrophosphatase	<i>EcPPase</i>	<i>Escherichia coli</i>	LB
Pyruvate decarboxylase	<i>ApPDC-var</i>	<i>Acetobacter pasteurianus</i>	AI

1.4. Protein production

1.4.1. Pre-culture

Twelve milliliters of LB medium were added to a 100 mL baffled, sterile Erlenmeyer flask. Next, ampicillin (100 mg mL⁻¹ stock solution) was added to a final concentration of 100 µg mL⁻¹. A colony was randomly picked from the agar plate containing the transformed cells (with a sterilized wooden or plastic stick) and dropped into the Erlenmeyer flask. This flask was incubated at 37 °C overnight at 150 rpm.

1.4.2. Production of carboxylate reductases in 1L-shaking cultures

A pre-culture, as described in 1.4.1, was started a day before the main cultivation. The main cultivation consisted of adding 1000 mL of TB medium and ampicillin (100 mg mL⁻¹ stock solution) to a final concentration of 100 µg mL⁻¹ into 6 x 5 L sterile, baffled Erlenmeyer flasks. Then, 5 mL of broth from the pre-culture was added in each flask, and the cultures were incubated at 37 °C, 90 rpm for 4 h. Subsequently, IPTG was added in each flask to a final concentration of 0.2 mM and the temperature was lowered to 15.6 °C. The cultivation was conducted for 48 h at 90 rpm. After 48 h, the cells were harvested by transferring the cell broth to 6 x 1 L Beckman centrifugal flasks (centrifugation conditions were 8000 rpm, 45 min, and 4 °C). The supernatants were discarded, the total cell mass was measured, and the overall pellet stored at -20 °C until further processing.

1.4.3. Production of whole-cell carboxylate reductases

NcCAR, *NiCAR* and *NoCAR* were produced as whole-cell catalysts in *E. coli* BL21(DE3), *E. coli* Tuner, and *E. coli* K-12 MG1655 RARE. The cultivation conditions in large scale shaking flasks were the same as described in 1.3. After harvesting, cells were stored at -20 °C until further use.

1.4.4. Production of ATP-regenerating enzymes and the pyrophosphatase from *E. coli*

The full regeneration of both ATP and NAD(P)H was achieved using the following auxiliary enzymes: the simultaneous action of polyphosphate kinases from *Meiothermus ruber* (*MrPPK*) and *Sinorhizobium meliloti* (*SmPPK*) for the regeneration of ATP and a glucose dehydrogenase (GDH) for the regeneration of NADPH. Finally, the inhibitory effects of pyrophosphate (PP), which is generated *in situ* during the catalytic cycle of CARs, is surpassed by using the pyrophosphatase from *Escherichia coli* (*EcPPase*). GDH from *Pseudomonas* sp. was commercially available and obtained from Sigma-Aldrich (Steinheim, Germany).

His-tagged *MrPPK* was used similarly as described previously by Parnell *et al.*⁹. *SmPPK* was expressed from the pET28+ vector constructed previously by Mordhorst *et al.*^{9,10} *E. coli* BL21 (DE3) served as the production host for all coenzymes used in this work. Cells were cultivated in LB medium and the expression of PPKs was induced by addition of 0.5 mM IPTG at 28 °C. Cell disruption and protein purification were performed as described for CARs.

Strep-tagged *EcPPase* was expressed from the pETSTREP3 vector as constructed previously by Pfeiffer *et al.*¹¹ Similarly, *E. coli* BL21(DE3) served as the expression host and was cultivated in LB medium at 37 °C. *EcPPase* expression was induced by addition of 0.5 mM IPTG. Purification was performed under standard conditions using a (i) Ni-NTA gravity flow column followed by (ii) a Strep-Tactin sepharose column as the stationary phase. Protein concentrations were determined with the Bradford assay.⁷

Full characterization of both PPKs and *EcPPase* in terms of enzyme activity was determined and described by Strohmeier *et al.*¹² Buffers used for protein purification are described in section 1.5.

1.4.5. Production of the (R)-selective pyruvate decarboxylase variant

E. coli BL21(DE3) cells containing a plasmid encoding for the pyruvate decarboxylase *ApPDC-var* were cultivated in AI medium. *ApPDC-var* was purified by Ni-NTA purification from crude cell extract (column material: Ni-NTA superflow, Qiagen, automated Äkta purifier system, GE Healthcare) and desalted and re-buffered by size exclusion chromatography (Sephadex G25 column). Purification buffers were as described in section 1.5. When used as whole-cell catalyst, the cultivation procedure was executed as stated previously but without the cell lysis and purification steps.

1.4.6. Production of transaminases

E. coli BL21(DE3) cells containing a plasmid encoding for transaminase *Cv2025* or for transaminase *BmTA* were cultivated in AI medium. Both transaminases were purified by Ni-NTA purification from crude cell extract (column material: Ni-NTA superflow, Qiagen, automated Äkta purifier system, GE Healthcare) and desalted and re-buffered by size exclusion chromatography (Sephadex G25 column). Buffers used for purification of *Cv2025* are listed in section 1.5. When used as whole-cell catalyst, the cultivation procedure was executed as stated previously but without the cell lysis and purification steps.

1.4.7. Production of the norcochlorine synthase variant $\Delta Tf29NCS-A79I$

E. coli BL21(DE3) was transformed with a pJ411 plasmid containing codon optimized $\Delta 29TfNCS-A79I$ by a standard heat-shock protocol, as described in the main manuscript. The grown colonies were used for cultivation of the cells in TB medium supplied with kanamycin and induced by 0.5 mM IPTG after 3-4 h (90 rpm, 20 °C). Cells were harvested and used for purification of the overexpressed $\Delta 29TfNCS-A79I$. The purification of the target protein was performed as described elsewhere.¹³ Buffers for protein purification are given in section 1.5. The lyophilised enzyme was stored at -20 °C. When used as whole-cell catalyst, the cultivation procedure was repeated as stated previously but without the cells lysis and purification steps.

1.5. Protein purification

For protein purification, target proteins were cultivated in large-scale shaking flask fermentation (6 x 1 L cultivation flasks). Subsequently, cells were mechanically lysed using a continuous ultra-sonication system (Hielscher UP200S, Sonotrode S1, 70% amplitude, 0.5 s cycle). For this, frozen cell pellets were first solubilized in the same equilibration buffer used for their purification, whose composition could differ depending on the target protein.

Tables S5 – S10 list all the solutions used for the purification of the different enzymes used in this work.

Table S5. Composition of buffer solutions for the purification of all carboxylate reductases

Buffer solutions	Components	Concentration (mM)
Equilibration buffer pH 7.0	Tris-HCl	50
	NaCl	1000
	Imidazole	10
Washing buffer pH 7.5	Tris-HCl	50
	NaCl	1000
	Imidazole	30
Elution buffer pH 7.5	Tris-HCl	50
	NaCl	1000
	Imidazole	250
Desalting buffer pH 7.0	Tris-HCl	10

Table S6. Composition of buffer solutions for the purification of the ATP-recycling enzymes *MrPPK* and *SmPPK*

Buffer solutions	Components	Concentration (mM)
Equilibration buffer pH 7.4	Tris-HCl	100
	NaCl	300
	Imidazole	10
Washing buffer pH 7.4	Tris-HCl	100
	NaCl	300
	Imidazole	30
Elution buffer pH 7.4	Tris-HCl	100
	NaCl	300
	Imidazole	250
Desalting buffer pH 7.4	Tris-HCl	20
	NaCl	150

Table S7. Composition of buffer solutions for the purification of the *EcPPase*

Buffer solutions	Components	Concentration (mM)
Equilibration buffer pH 7.4	Tris-HCl	100
	NaCl	300
	Imidazole	10
Washing buffer pH 7.4	Tris-HCl	100
	NaCl	300
	Imidazole	20
Elution buffer pH 7.4	Tris-HCl	100
	NaCl	300
	Imidazole	250
Buffer W pH 8.0	Tris-HCl	100
	NaCl	150
	EDTA	1
Buffer E pH 8.0	Tris-HCl	100
	NaCl	150
	EDTA	1
	D-Desthiobiotin	2.5

Buffers W and E were used for the Strep-tactin chromatography directly after the Ni-NTA chromatography.

Table S8. Composition of buffer solutions for the purification of the pyruvate decarboxylase *ApPDC-var*

Buffer solutions	Components	Concentration (mM)
Equilibration buffer pH 7.0	Tris-HCl	100
	NaCl	300
	Imidazole	10
	ThDP	0.1
	MgSO ₄	2.5
Washing buffer pH 7.5	Tris-HCl	100
	NaCl	300
	Imidazole	30
	ThDP	0.1
	MgSO ₄	2.5
Elution buffer pH 7.5	Tris-HCl	100
	NaCl	300
	Imidazole	250
	ThDP	0.1
	MgSO ₄	2.5
Desalting buffer pH 7.0	Tris-HCl	10
	ThDP	0.1
	MgSO ₄	2.5

Table S9. Composition of buffer solutions for the purification of the amine transaminases *BmTA* and *Cv2025*

Buffer solutions	Components	Concentration (mM)
Equilibration buffer pH 7.0	Tris-HCl	100
	NaCl	300
	Imidazole	10
	PLP	0.2
Washing buffer pH 7.5	Tris-HCl	100
	NaCl	300
	Imidazole	30
	PLP	0.2
Elution buffer pH 7.5	Tris-HCl	100
	NaCl	300
	Imidazole	250
	PLP	0.2
Desalting buffer pH 7.0	Tris-HCl	10
	PLP	0.2

Table S10. Composition of buffer solutions for the purification of the norcochlorine synthase $\Delta Tf29NCS-A79I$

Buffer solutions	Components	Concentration (mM)
Equilibration buffer pH 7.5	Tris-HCl	100
	NaCl	300
	Imidazole	20
Washing buffer pH 7.5	Tris-HCl	100
	NaCl	300
	Imidazole	40
Elution buffer pH 7.5	Tris-HCl	100
	NaCl	300
	Imidazole	500
Desalting buffer pH 7.5	Tris-HCl	10

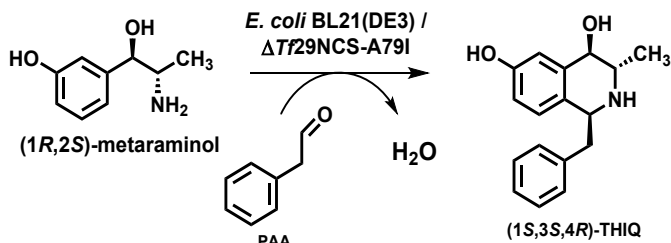
1.6. Determination of initial rates of CARs

The determination of initial rate of CAR enzymes was performed using a NADPH photometric-based assay. For the assay, ATP and NADPH were freshly dissolved in ultrapure water. The substrates sodium benzoate (NaBZ), 3-hydroxybenzoic acid (3-OH-BZ), and 4-hydroxybenzoic acid (4-OH-BZ) were solubilized in 100 mM KOH. Protocatechuic acid (PCA) was solubilized in a mixture composed by 100 mM KOH and DMSO. Purified, lyophilised CAR enzymes were dissolved in the assay buffer. The total volume of the assay was 1 mL and its composition was as follows: 100 mM Tris-HCl buffer pH 7.5 (200 mM in water, containing 1 mM 1,4-dithiothreitol and 1 mM ethylenediaminetetraacetic acid), 10 mM substrate (100 mM in 100 mM KOH, DMSO or a mixture), 30 mM MgCl₂ (300 mM in water), 1 mM ATP (20 mM in water), 0.045 mM NADPH (1 mM in water). Subsequently, the measurement started after the addition of enzyme (100 μL from the enzyme stock). The protein content of the enzyme stock was determined by Bradford assay.⁷ The depletion of NADPH was followed on semi-micro PMMA cuvettes using a spectrophotometer (Shimadzu UV-1800 spectrophotometer, Switzerland) at 340 nm and 30 °C for 2 min, similarly as described elsewhere.⁷ Each assay was carried out in technical triplicates and the results were shown as average values. One enzyme unit (U) was defined as the amount of enzyme that consumed one μmol of NADPH per min under the applied assay conditions. The volumetric activity (in U mL⁻¹) and specific activity (in U mg⁻¹) were determined as described elsewhere.⁷

2. Enzymatic production of compound standards

2.1. (1*S*,3*S*,4*R*)-1-Benzyl-3-methyl-1,2,3,4-tetrahydroisoquinoline-4,6-diol

The standard compound (1*S*,3*S*,4*R*)-1-benzyl-3-methyl-1,2,3,4-tetrahydroisoquinoline-4,6-diol or (1*S*,3*S*,4*R*)-THIQ was synthesised starting with the commercially available (1*R*,2*S*)-metaraminol bitartrate, as shown in Scheme S1.



Scheme S1. Reaction scheme for the larger scale synthesis of (1*S*,3*S*,4*R*)-THIQ catalyzed by Δ*Tf29NCS-A79I* as whole cell catalyst.

Two independent reactions (200 mL) were conducted in a 500 mL stirred glass reactor (EasyMax 402, Mettler Toledo; Columbus, USA), in which 100 mM HEPES pH at 7.5 were added, followed by 15 mM (1*R*,2*S*)-metaraminol bitartrate. Subsequently, 15 mM phenylacetaldehyde and 10 g L⁻¹ lyophilized *E. coli* BL21 (DE3) cells expressing Δ*Tf29NCS-A79I* were added. Phenylacetaldehyde was supplied two additional times (15 mM each time and added as pure compound) to guarantee maximal conversion of the substrate. Reactions were carried out at 30 °C and 300 rpm until full conversion was achieved (up to 24 h). For the work-up, a 1 M HCl solution was added (20 mL) and the mixture was centrifuged at 4000 rpm for 10 min.

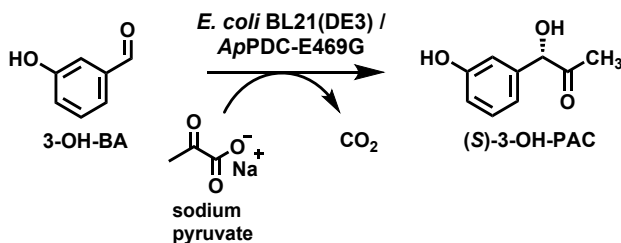
Next, the supernatant had its pH adjusted to 7.5 and it was extracted three times with 200 mL ethyl acetate. Subsequently, the organic phases were combined and dried out with MgSO₄. To facilitate the evaporation of the solvent, the organic phase was rota-evaporated in small fractions (50 – 100 mL) at 40 °C and 100 mbar. The obtained solid was washed with a 5:1 (v v⁻¹) mixture of petrol ether and ethyl acetate (1 x 50 mL). The solid was filtered and left to dry for NMR analysis.

2.2. (1S,3S,4S)-1-Benzyl-3-methyl-1,2,3,4-tetrahydroisoquinoline-4,6-diol

The compound (1S,3S,4S)-1-benzyl-3-methyl-1,2,3,4-tetrahydroisoquinoline-4,6-diol was synthesised to use as a standard to quantify it in case it would be formed during the cyclisation reaction (last reaction step, Scheme 1 of the main manuscript). It is important to mention that this is not the main product of the cyclisation reaction described in the main manuscript, but it could be formed in tiny amounts due to background activity. Therefore, in order to determine the isomeric content (see more details in section 4), all possible stereoisomers should be quantified. Other stereoisomers were described in Erdman et al (2017).¹³

2.2.1. (S)-3-Hydroxyphenylacetylcarbinol

(S)-3-hydroxyphenylacetylcarbinol, or (S)-3-OH-PAC, was performed as shown in Scheme S2.



Scheme S2. Reaction scheme for the larger scale synthesis of (S)-3-OH-PAC catalyzed by the (S)-selective ApPDC-E469G¹⁴ as whole-cell catalyst.

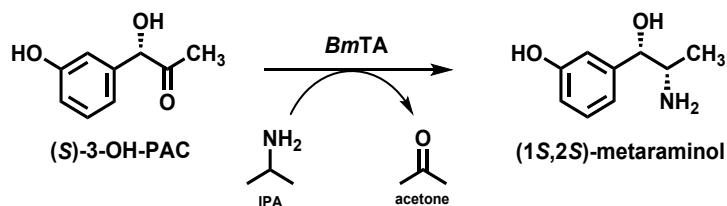
(S)-3-OH-PAC was synthesized and purified to serve as starting material to produce (1S,2S)-metaraminol and, subsequently, (1S,3S,4S)-THIQ. Larger reaction (400 mL) for the production of (S)-3-OH-PAC were performed in a 600 mL stirred-tank reactor (EasyMax 402, Mettler Toledo; Columbus, US) including pH control. Eventually, the pH was manually adjusted by the addition of 1 M NaOH. The reaction conditions were as follows: 100 mM HEPES at pH 6.5, 60 mM 3-OH-BA, 300 mM sodium pyruvate, 1 mM ThDP, 4 mM MgSO₄, 10 g L⁻¹ lyophilized *E. coli* BL21(DE3) cells with heterologously produced ApPDC-E469G. Reaction was carried out at 30 °C and 350 rpm until full conversion was achieved (about 5 h). Conversions were monitored by HPLC analysis. The (S)-selective ApPDC-E469G was produced according to procedures published elsewhere.^{14,15}

For the reaction work-up, a solution of 20% (w/v) HCl was added and the mixture centrifuged at 4000 rpm for 10 min. Subsequently, the pH was adjusted to 7.5 and the supernatant was extracted with ethyl acetate (4 x 200 mL). Before filtration, MgSO₄ was added as a drying agent. Eventually, the addition of this

salt also ease the precipitation of remaining cell debris. The organic phase was evaporated and the obtained solid was washed with a 5:1 mixture of petrol ether and ethyl acetate (1 x 50 mL) to eluate any remaining impurity. Then, the solid was filtered under vacuum. Approximately, 1.6 g of solid product was obtained.

2.2.2. 3-((1*S*,2*S*)-2-Amino-1-hydroxypropyl)phenol

3-((1*S*,2*S*)-2-Amino-1-hydroxypropyl)phenol, or (1*S*,2*S*)-metaraminol, was synthesised as shown in Scheme S3.

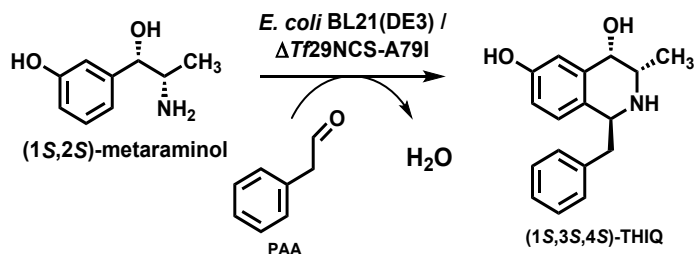


Scheme S3. Reaction scheme for the larger scale synthesis of (1*S*,2*S*)-metaraminol catalyzed by the (*S*)-selective *BmTA*.

For the synthesis, (*S*)-3-OH-PAC produced and purified in the previous step served as substrate following a similar setup, as described previously. Larger reaction (200 mL) to produce (1*S*,2*S*)-metaraminol were performed in a 600 mL stirred-tank reactor (EasyMax 402), including pH control. Reaction conditions were as follows: 100 mM HEPES at pH 7.5, 15 mM (*S*)-3-OH-PAC added as solid, 25 mM IPA, 1 mM PLP, 1 g L⁻¹ purified and lyophilized *BmTA*. IPA was eventually supplied 2 or 3 additional times to guarantee maximal conversion of the substrate. Reaction was carried out at 30 °C and 300 rpm until >95% conversion was achieved (about 4 h). Conversions were monitored by HPLC analysis. The solution was centrifuged (4000 rpm, 30 min) to get rid of the precipitated protein. Next, the solution was filtered using a 30 kDa cut-off membrane centrifugal tube. The colourless supernatant was directly used in the next step.

2.2.3. (1*S*,3*S*,4*S*)-1-Benzyl-3-methyl-1,2,3,4-tetrahydroisoquinoline-4,6-diol

(1*S*,3*S*,4*S*)-1-Benzyl-3-methyl-1,2,3,4-tetrahydroisoquinoline-4,6-diol, or (1*S*,3*S*,4*S*)-THIQ, was synthesized starting with the supernatant from the previous step, which contained (1*S*,2*S*)-metaraminol, according to Scheme S4.



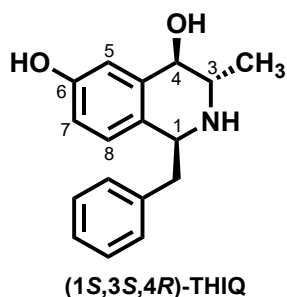
Scheme S4. Reaction scheme for the larger scale synthesis of (1*S*,3*S*,4*S*)-THIQ catalyzed by $\Delta 297fNCS$ -A79I as whole cell catalyst.

Larger reaction (200 mL) were setup in a 600 mL stirred-tank reactor (EasyMax 402). Reaction conditions were as follows: 200 mL from the previous step, 15 mM phenylacetaldehyde (PAA), and 1 g L⁻¹ purified, lyophilized $\Delta 297fNCS$ -A79I or 10 g L⁻¹ lyophilized *E. coli* BL21 (DE3) cells with heterologously produced $\Delta 297fNCS$ -A79I. Phenylacetaldehyde (PAA) was supplied 2 or 3 additional times to guarantee maximal conversion of the substrate. Reaction was carried out at 37 °C and 300 rpm until full conversion was achieved (up to 24 h). Conversions were monitored by HPLC analysis. The crude product assumes a yellow coloration, which can be diminished by conducting the reaction at 30 °C instead. This makes the reaction a bit slower; however, the yellow coloration is becomes less prominent, facilitating the product isolation and purification.

For the reaction work-up, a 1 M HCl solution was added (20 mL) and the mixture was centrifuged at 4000 rpm for 10 min. Next, the pH of the supernatant was adjusted to 7.5 and it was extracted with ethyl acetate (3 x 200 mL). Subsequently, the organic phases were combined and dried out with MgSO₄. To facilitate the evaporation of the solvent, the organic phase was rota-evaporated in small fractions (50 – 100 mL). The obtained solid could have a yellowish color, which was diminished by washing it with a 5:1 mixture of petrol ether and ethyl acetate (1 x 50 mL). The solid was filtered and left to dry for NMR analysis.

2.3. NMR data

2.3.1. (1*S*,3*S*,4*R*)-THIQ



¹H NMR (700 MHz; CD₃OD) δ 7.34–7.24 (m, 5H, 2 x Ph 2-H, 2 x Ph 3-H, Ph 4-H), 6.98 (d, J = 2.7 Hz, 1H, 5-H), 6.90 (d, J = 8.4 Hz, 1H, 8-H), 6.63 (dd, J = 8.4, 2.7 Hz, 1H, 7-H), 4.15 (d, J = 8.6 Hz, 1H, 4-H), 4.08 (dd, J = 8.8, 5.6 Hz, 1H, 1-H), 3.15 (dq, J = 8.6, 6.3 Hz, 1H, 3-H), 3.07 (dd, J = 13.7, 8.8 Hz, 1H, CHHPh) 3.04 (dd, J = 13.7, 5.6 Hz, 1H, CHHPh), 1.18 (d, J = 6.3 Hz, 3H, CH₃);

¹³C NMR (176 MHz; CD₃OD) δ 157.3, 140.1, 140.08, 130.3, 129.7 (signals superimposed), 128.7, 127.6, 115.4, 114.4, 73.4, 57.8, 50.4, 43.4, 18.6.

YNS3.10.fid
PROTON, MeOD (C:\700) hch 55

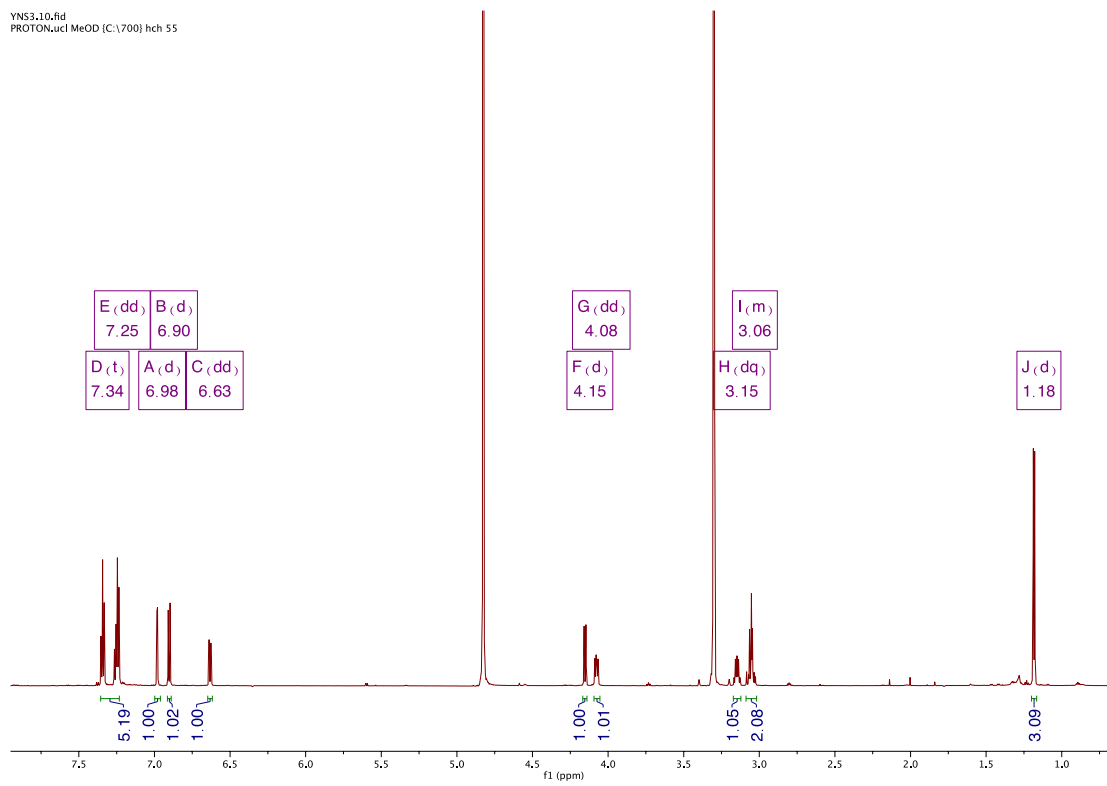


Figure S1. ¹H-NMR

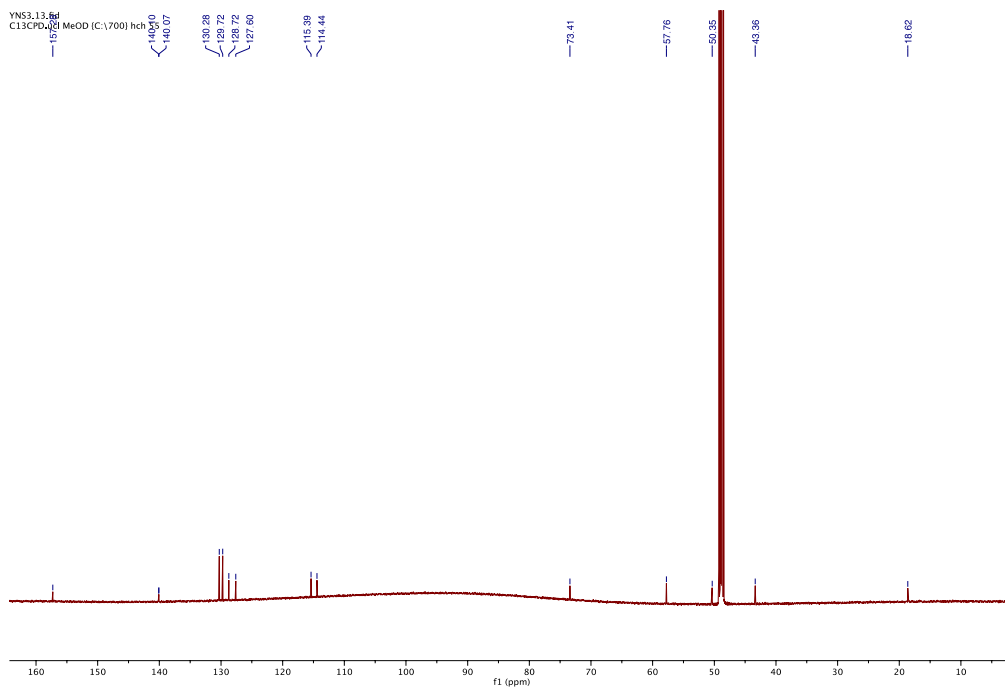


Figure S2. ¹³C-NMR

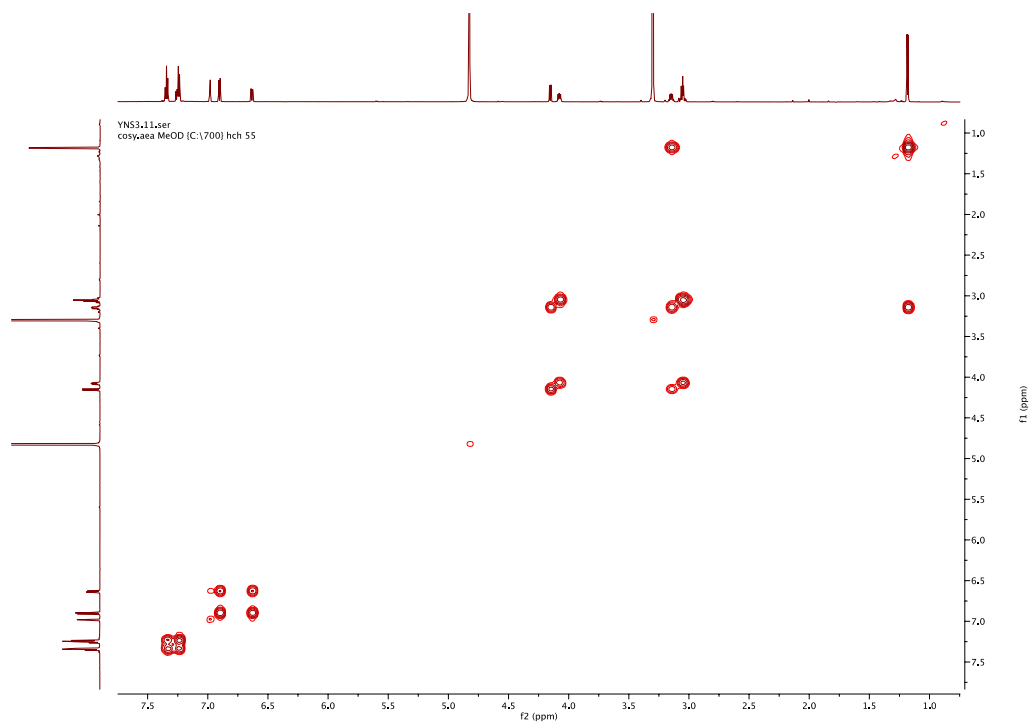


Figure S3. ^1H - ^1H COSY

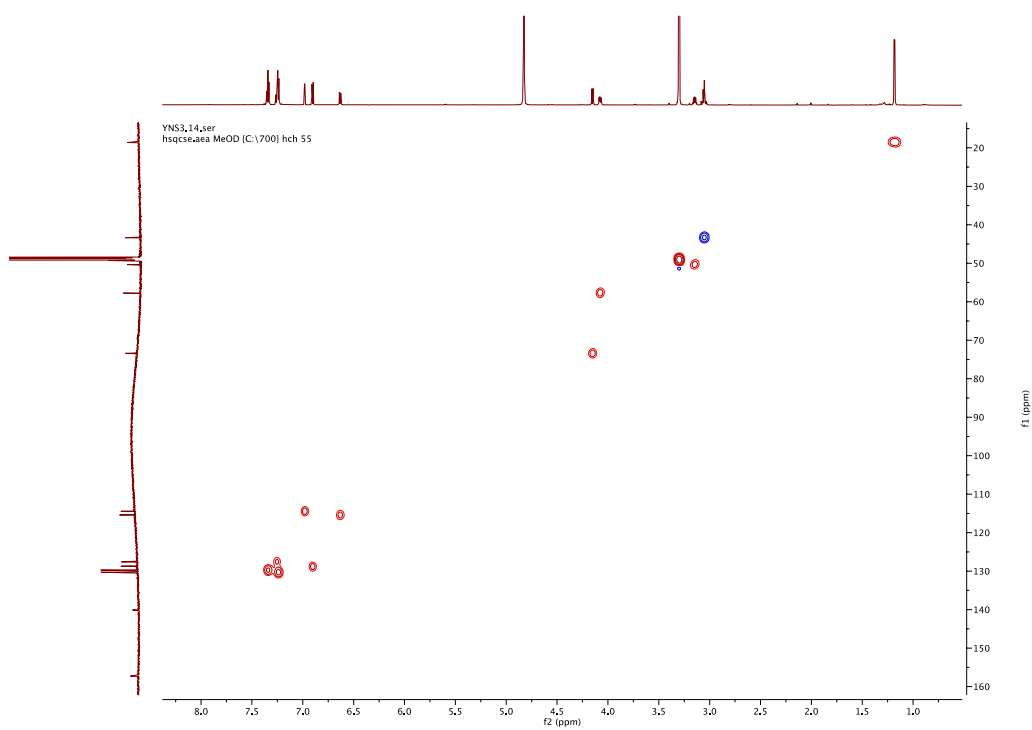


Figure S4. HSQC

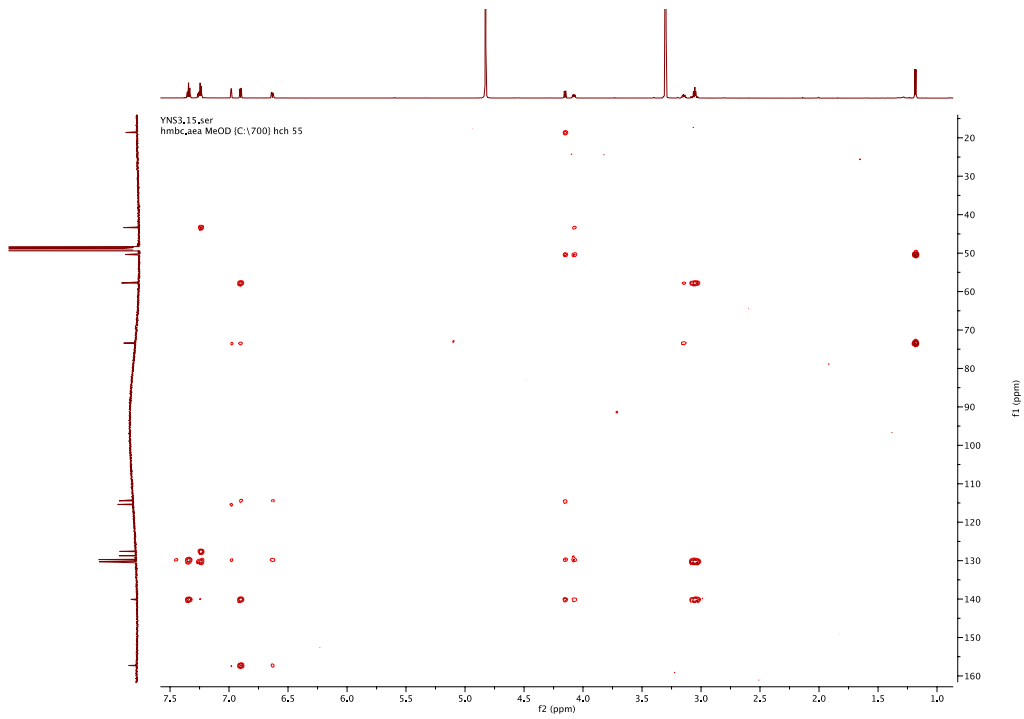


Figure S5. HMBC

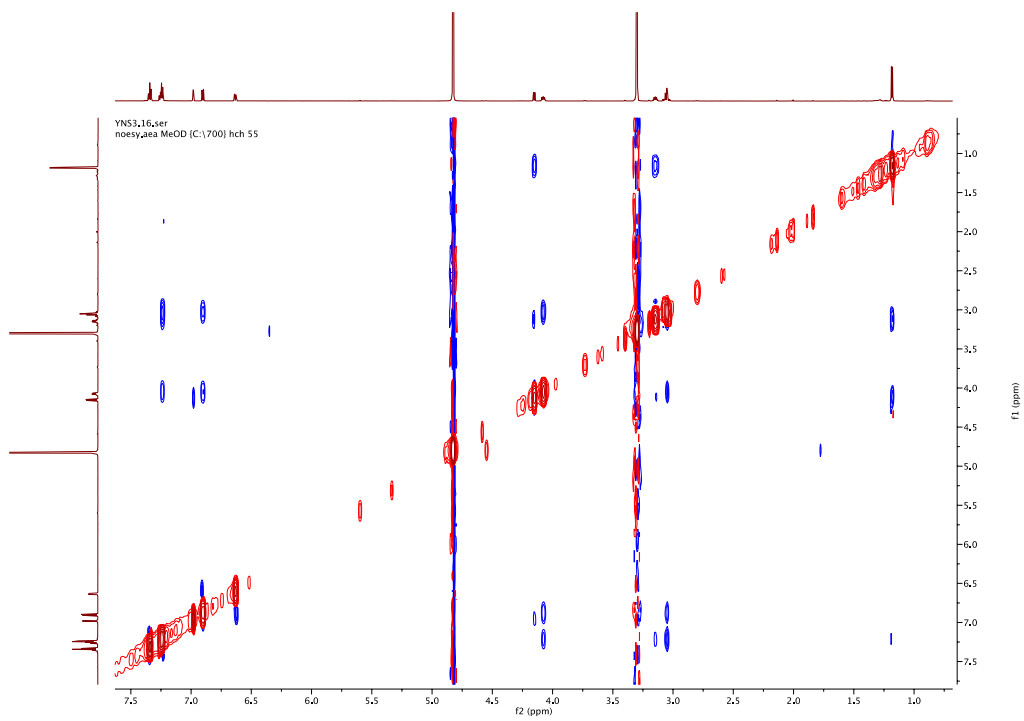
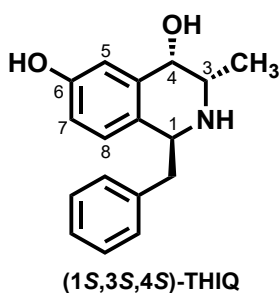


Figure S6. NOESY

Key NOEs (S strong; M medium; W weak):

1-H	8-H, 9-H S ; 4-H W
3-H	3-Me S ; 9-H M ; 4-H, Ph ortho-H W ; 1-H, 5-H vW
3-Me	3-H, 4-H S ; Ph ortho-H W ; 1-H vW
4-H	3-Me, 5-H S ; 3-H, 1-H W

2.3.2. (1S,3S,4S)-THIQ



Mp 224–226°C (methanol); $[\alpha]_D^{20}$ 36.0 (c 0.067, MeOH); $^1\text{H NMR}$ (700 MHz; CD_3OD) δ 7.30–7.35 (m, 3H, 2 x Ph 3-H, Ph 4-H), 7.18 (m, 2H, 2 x Ph 2-H), 6.83 (d, $J = 2.5$ Hz, 1H, 5-H), 6.72 (d, $J = 8.5$ Hz, 1H, 8-H), 6.69 (dd, $J = 8.5, 2.5$ Hz, 1H, 7-H), 4.72 (app. t, $J = 7.0$ Hz, 1H, 1-H), 4.53 (d, $J = 2.6$ Hz, 1H, 4-H), 3.66 (qd, $J = 6.7, 2.6$ Hz, 1H, 3-H), 3.24–3.30 (dd, $J = 14.0, 7.5$ Hz, 1H, CHHPh) 3.24 (dd, $J = 14.0, 6.5$ Hz, 1H, CHHPh), 1.39 (d, $J = 6.7$ Hz, 3H, CH_3);

$^{13}\text{C NMR}$ (176 MHz; CD_3OD) δ 158.7, 137.3, 136.7, 130.7, 130.0, 129.3 (2 superimposed signals), 128.7, 122.2, 116.9, 116.9, 67.2, 57.4, 50.9, 41.2, 14.5; m/z [ES+] 270 ([MH]⁺, 100%); m/z [HRMS ES+] found [MH]⁺ 270.1488. $\text{C}_{17}\text{H}_{20}\text{NO}_2$ requires 270.1488.

YNS1.11.fid
PROTON,ulc MeOD (C:1700) hch 8

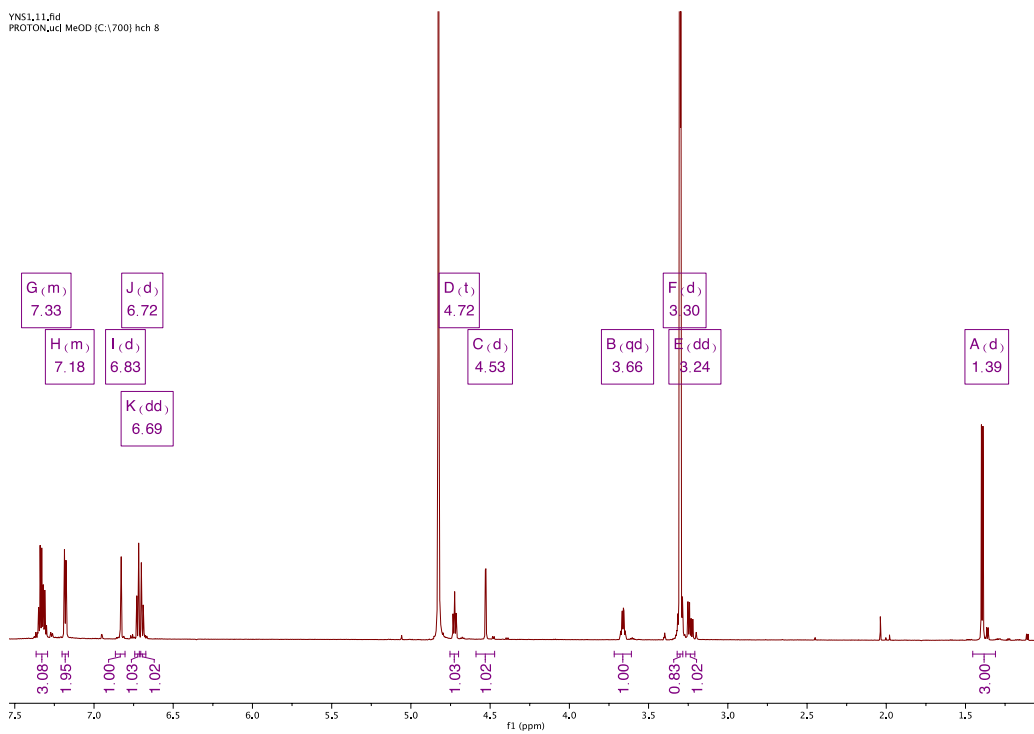


Figure S7. ¹H-NMR

YNS1.12.fid
C13CPD,ulc MeOD (C:1700) hch 8

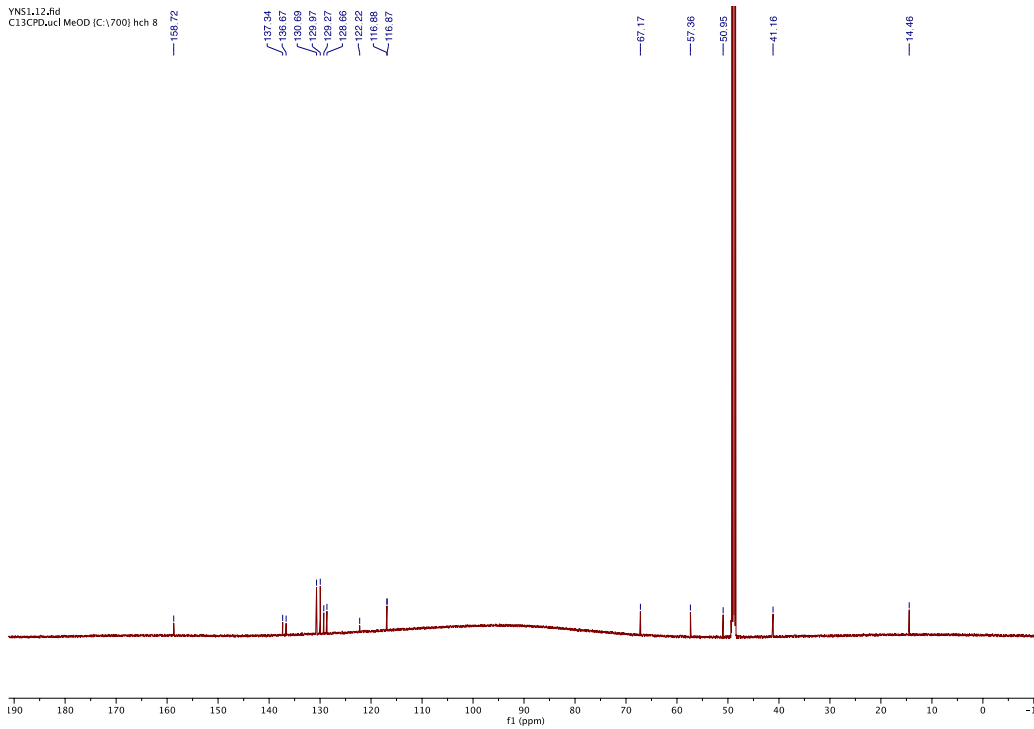


Figure S8. ¹³C-NMR

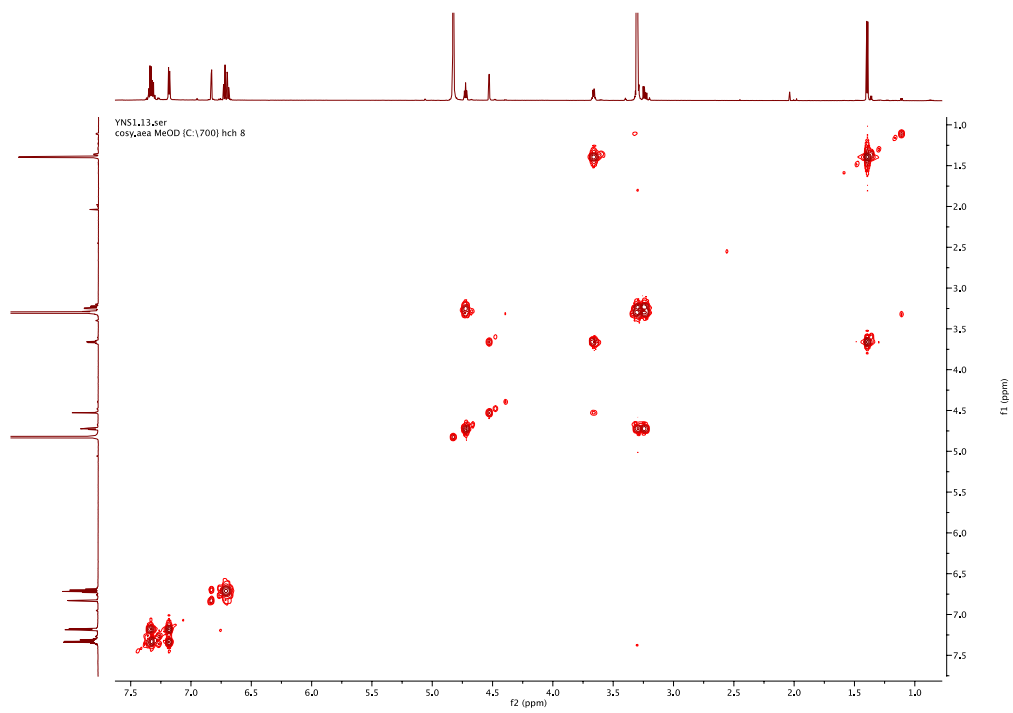


Figure S9. ¹H-¹H COSY

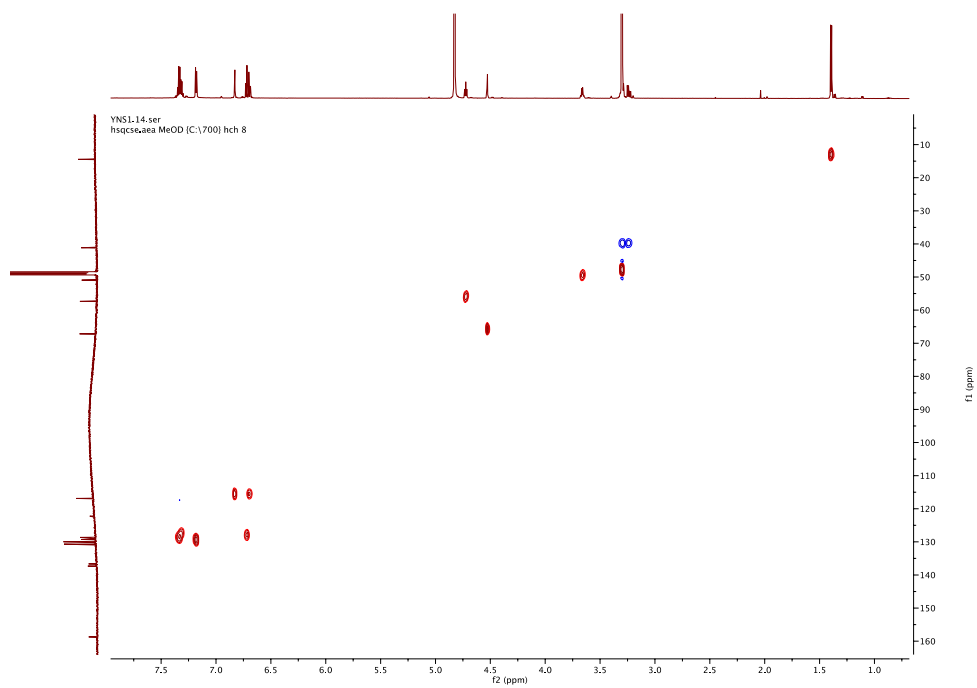


Figure S10. HSQC

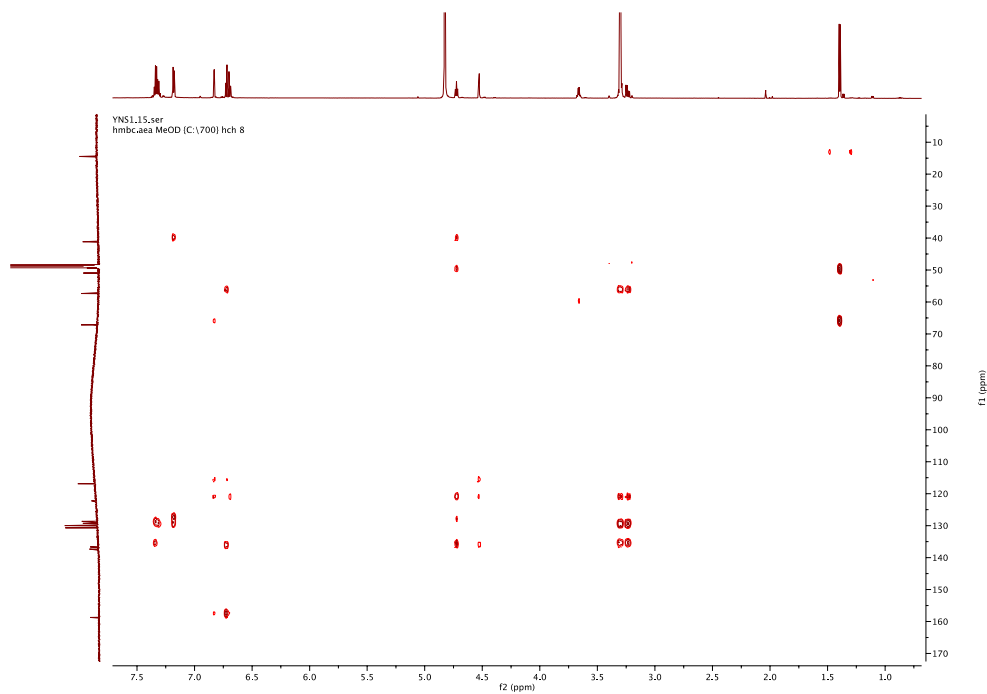


Figure S11. HMBC

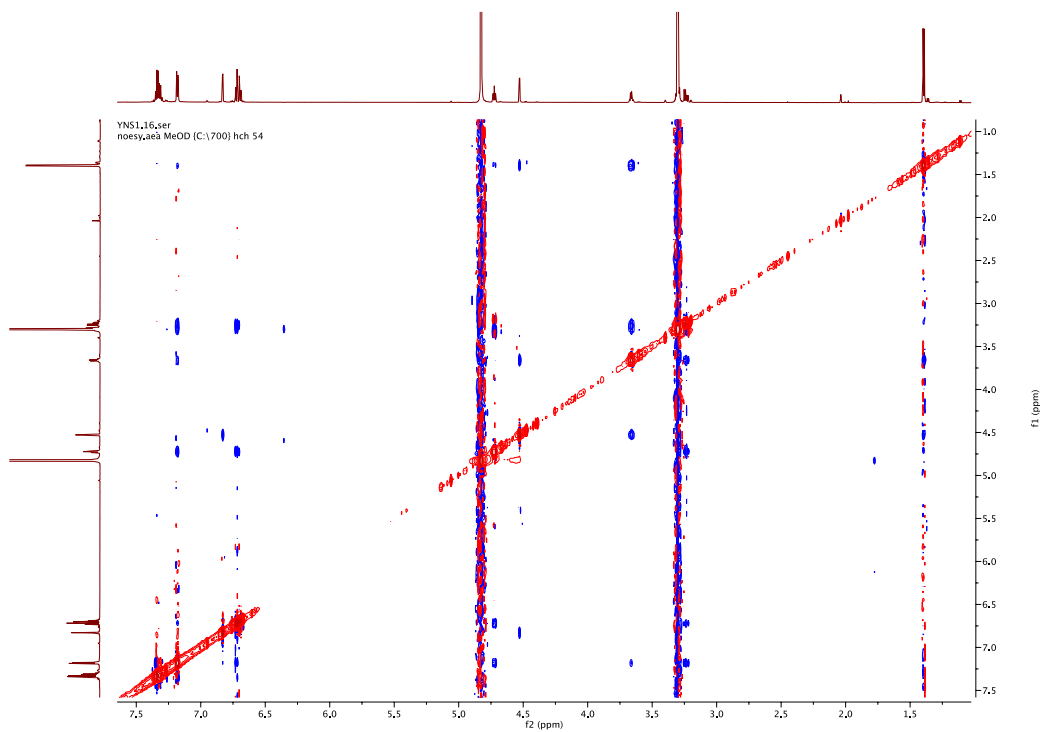


Figure S12. NOESY

Key NOEs (S strong; M medium; W weak):

1-H	8-H, 9-H S ; 7-H W ; 3-H, 4-H very W
3-H	3-Me, 4-H S ; 9-H M ; Ph <i>ortho</i> -H W
3-Me	3-H S ; 4-H M ; 1-H, Ph <i>ortho</i> -H W
4-H	5-H S ; 3-H, 3-Me M

3. HPLC analytics

3.1. Method I

The analysis of (hydroxy)benzoates and their corresponding aldehydes and alcohols was carried out in a HPLC Agilent 1100 TC Thermo G1 equipped with a Diode Array Detector (DAD) and an Agilent XDB – C18 column. The mobile phases were as follows: solvent A composed by 100% acetonitrile (ACN) and solvent B composed by ammonium acetate (5 mM) and 0.5% v/v acetic acid in water. A stepwise gradient at a flow rate of 1.0 mL min⁻¹ was used: 10–50% ACN (5 min) and 50–90% ACN (5.0–9.0 min). The total run time was 10 min. After additional 30 s, the column was re-equilibrated to the starting conditions. The compounds were detected at 254 nm.

Calibration curves were determined at 254 nm and linear interpolation used for their quantification. In addition, ethyl *p*-hydroxybenzoate (stock solution of 0.5 mg mL⁻¹ in acetonitrile) was used as internal standard for constructing the external calibration curves and measuring samples in the HPLC.

For the analysis, samples from the reaction mixture (30 – 50 µL) were taken over time and the reaction stopped by the addition of a quenching solution (ACN/formic acid at 19:1 ratio). Dilutions of 1:5, 1:10 or 1:20 with quenching solution were applied depending on the starting concentration of substrate. Subsequently, samples were centrifuged (*ca.* 20000 x *g*/14600 rpm, 5 min, 4 °C) and 100 µL were transferred to HPLC vials for the measurement. The retention time of the compounds analyzed *via* this method are listed in Table S11.

Table S11. Retention time of compounds detected *via* HPLC method I

Compound	Retention time (min)
4-hydroxybenzyl alcohol	2.3
3-hydroxybenzyl alcohol	2.8
3,4-dihydroxybenzyl alcohol	1.9
4-hydroxybenzoic acid	3.2
3-hydroxybenzoic acid	3.6
protocatechuic acid	2.3
4-hydroxybenzaldehyde	4.0

3-hydroxybenzaldehyde	4.2
3,4-dihydroxybenzaldehyde	3.1
benzyl alcohol	4.2
sodium benzoate	5.0
benzaldehyde	5.8
<i>p</i> -ethyl paraben	6.2

3.2. Method II

A second method was developed for the quantitative analysis of (*R*)-3-OH-PAC and (1*R*,2*S*)-metaraminol. In addition, this method was eventually used (as an alternative to method I) for the quantitative analysis of 3-OH-BZ, 3-OH-BA, 3-OH-benzyl alcohol, PCA, 3,4-dihydroxybenzaldehyde, 3,4-dihydroxybenzyl alcohol, and THIQ. As this method does not include a chiral column, the analysis of the compounds mentioned was purely quantitative without differentiation of enantiomers. Therefore, chiral compounds were fully characterized using the method III (next section).

In this method, samples (10 μ L) were injected into the HPLC device and analyzed by a reversed phase chromatography column (LiChrospher® 100 RP-18, Merck KGaA). The gradient elution was done with solvent A (acetonitrile + 0.1% TFA) and solvent B (ddH₂O + 0.1% TFA) with a flow rate of 0.5 mL min⁻¹. The total run time was 25 min. The concentration (mM) of the compounds was automatically calculated by the HPLC software (Chromeleon™ 7.2) using individual external calibration curves for each compound. The retention times are listed on the Table S12.

Table S12. Retention time of compounds detected *via* HPLC method II

Compound	Retention time (min)
3,4-dihydroxyphenylacetylcarbinol	10.6
(1 <i>R</i> ,2 <i>S</i>)-metaraminol	10.6
(1 <i>S</i> ,2 <i>S</i>)- metaraminol	10.6
3,4-dihydroxybenzyl alcohol	11.4
3-hydroxybenzyl alcohol	11.9
3,4-dihydroxybenzaldehyde	12.4
(<i>R</i>)-3-hydroxyphenylacetylcarbinol	12.5
(<i>S</i>)-3-hydroxyphenylacetylcarbinol	12.5
3-hydroxybenzoic acid	13.2
(1 <i>R</i> ,3 <i>S</i> ,4 <i>S</i>)-THIQ	14.3
(1 <i>S</i> ,3 <i>S</i> ,4 <i>S</i>)-THIQ	14.3
3-hydroxybenzaldehyde	14.5

Sampling consisted on pipetting 20 – 50 μ L of reaction mixture into a stop solution (ACN + 0.1% trifluoroacetic acid) to quench the reaction. Samples were diluted 1:5, 1:10 or 1:20 (depending on the

substrate starting concentration) and centrifuged for 5 min (*ca.* 20000 x *g* or 14600 rpm). Next, 100 μ L were transferred into HPLC vials and analyzed according to the described method.

3.3. Method III

This method was used to determine both the stereopurity of metaraminol as well as the reaction progress of the cyclization step, including the determination of the stereopurity of the THIQ product. For this, samples (5 μ L) were injected in the HPLC column (Crownpak CR-I (+) Diacel, 150 mm x 3 mm x 5 μ m) and eluted isocratically using a 0.1 M HClO₄/ACN (80/20, volume percent) solution as the mobile phase at a flow rate of 0.3 mL min⁻¹. The total run time was 20 min.

For sample preparation, 20 - 100 μ L of the reaction mixture was quenched by an aqueous 0.24 M HCl solution (2% of the 37% stock) with dilution factors of 1:2, 1:4 or 1:10. Next, samples were centrifuged (*ca.* 20000 x *g*/14600 rpm) and analysed. Compounds were detected and quantified at 210 nm. The retention times are listed in Table S13.

Table S13. Retention time of compounds detected *via* HPLC method III

Compound	Retention time (min)
DMSO	3.7
(<i>R</i>)-3-hydroxyphenylacetylcarbinol	5.6
(<i>S</i>)-3-hydroxyphenylacetylcarbinol	5.6
(1 <i>S</i> ,2 <i>S</i>)- metaraminol	6.2
(1 <i>R</i> ,2 <i>S</i>)-metaraminol	6.7
phenylacetaldehyde	8.2
3-hydroxybenzaldehyde	9.3
(1 <i>S</i> ,3 <i>S</i> ,4 <i>R</i>)-THIQ	9.7
(1 <i>S</i> ,2 <i>R</i>)-metaraminol	11.7
(1 <i>S</i> ,3 <i>S</i> ,4 <i>S</i>)-THIQ	10.8
phenylethylamine	17

3.4. Method IV

This method was only used to confirm the stereopurity of the (*R*)-3-OH-PAC enzymatically produced in the carbologation reaction catalysed by *Ap*PDC-E469Q. This method includes a 2D analysis of a pre-selected peak (*i.e.*, at a fixed retention time) which was analysed using a 1D setup. The 2D analysis (UHPLC

system, Agilent Infinity 1290 II, Agilent Technologies, Santa Clara, USA) allows to distinguish between enantiomers of the same compound. The method specifications were as follows:

- 1D analysis: 10 – 90% ACN gradient in 5 min (6 min total), at a flow rate of 0.5 mL min⁻¹; 20 °C, 5 µL injection volume. Sample were injected into a Zorbax Eclipse plus C18, 2x100 mm, 1.8 µm column (with Zorbax RRHD Eclipse plus C18 guard column).
- 2D analysis: Heart-cutting, 10-90% ACN in 3 min flow rate of 0.6 mL min⁻¹, 3.5 min cycle time⁻¹; 1.95 min time-based cut, 0.08 min sampling time, Loop filling > 300 %, 2D column ratio 38%. The column used in the 2D analysis was Chiralpak IE-3, 2x100 mm, 3 µm, with detection at 254 nm and temperature of analysis of 20 °C.

Samples from enzyme reactions were diluted 1:20 or 1:40 in 50% v v⁻¹ acetonitrile (ACN) and mixed thoroughly to stop the reaction process and precipitate dissolved proteins. The sample was centrifuged at 13,000 rpm for 4 min and the supernatant was used for HPLC analysis (retention time of 3-OH-PAC = 1.99 min).

4. Determination of process metrics

Process metrics were determined as follows.

Reaction conversion: the enzymatic conversion was calculated as shown in Eq. 1:

$$\text{Conversion (\%)} = \frac{[\text{substrate}]_0 - [\text{substrate}]_t}{[\text{substrate}]_0} * 100 \quad (1)$$

in which $[\text{substrate}]_0$ is the initial substrate concentration and $[\text{substrate}]_t$ is the concentration of substrate after certain time t of reaction determined via HPLC analytics.

Product yield (or HPLC yield): the formation of product in terms of HPLC yield (%), was calculated as shown in Eq. 2:

$$\text{HPLC yield (\%)} = \frac{[\text{product}]_t}{[\text{substrate}]_0} * 100 \quad (2)$$

in which $[\text{product}]_t$ is the concentration of product formed after certain time t of reaction. Formation of products and depletion of substrates in terms of concentration (mM) were calculated using calibration curves built using purchased or synthesized standard compounds.

Enantiomeric excess (ee): is a measurement of purity used for chiral substances and it was determined using the Eq. 3:

$$ee (\%) = \frac{[E]_1 - [E]_2}{[E]_1 + [E]_2} * 100 \quad (3)$$

in which $[E]_1$ is the concentration of enantiomer 1 (or its area under the peak on the HPLC chromatogram) and $[E]_2$ is the concentration of enantiomer 2 (or its area under the peak on the HPLC chromatogram).

Isomeric content (ic):¹⁶ to compare two-step reactions more easily, the content of the target isomer (isomeric content, ic) of a reaction is given as the percent fraction of the target isomer in a mixture of all stereoisomers detected (whether enantiomer or diastereoisomer), as shown in Eq. 4:

$$ic (\%) = \frac{[I]_1}{\sum [I]_i} * 100 \quad (4)$$

in which $[I]_1$ is the concentration of stereoisomer 1 (or its area under the peak on the HPLC chromatogram) and $[I]_i$ is the concentration of isomer i (or its area under the peak on the HPLC chromatogram).

5. Supporting data

5.1. Substrate scope investigation of CAR enzymes

A small toolbox of CARs was first characterized by the determination of their initial rates. The photometric-based assay used to determine initial rate of CARs was the depletion of NADPH at 340 nm, as described in section 1.6. The following heat map shows the results obtained in this study.

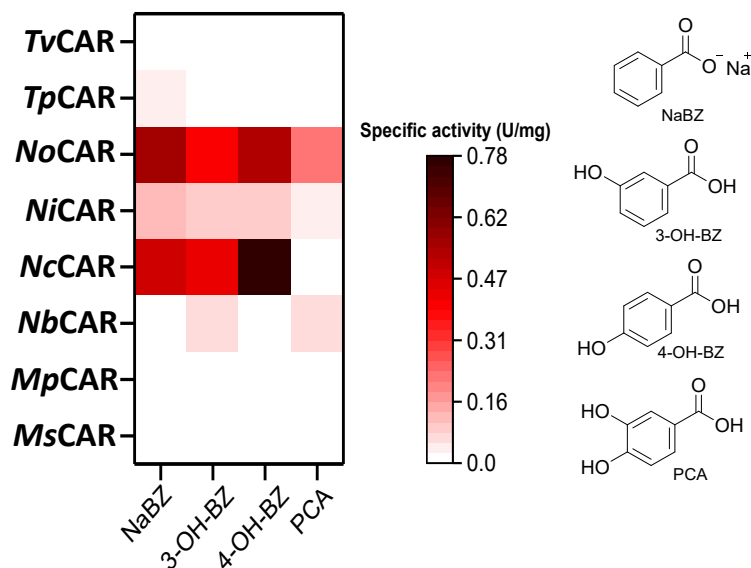


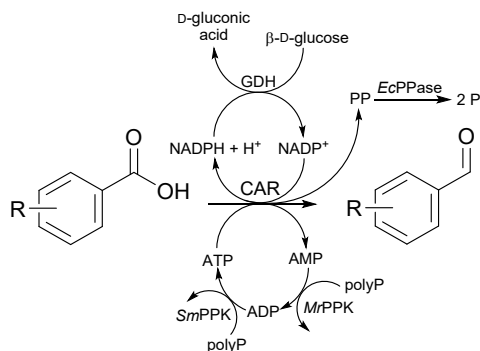
Figure S13. Initial rate of purified CARs towards several (hydroxy)benzoates, as follows: sodium benzoate (NaBZ), 3-hydroxybenzoic acid (3-OH-BZ), 4-hydroxybenzoic acid (4-OH-BZ), and protocatechuic acid (PCA). CAR enzymes used in this work: carboxylate reductase from *Trametes versicolor* (TvCAR), carboxylate reductase from *Tsumakurella paurometabola* (TpCAR), carboxylate reductase from *Nocardia otitidiscaviarum* (NoCAR), carboxylate reductase

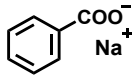
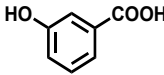
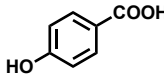
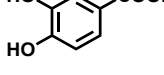
from *Nocardia iowensis* (NiCAR), carboxylate reductase from *Neurospora crassa* (NcCAR), carboxylate reductase from *Nocardia brasiliensis* (NbCAR), carboxylate reductase from *Mycobacterium phlei* (MpCAR), carboxylate reductase from *Mycobacterium smegmatis* (MsCAR).

As can be observed, NoCAR, NiCAR and NcCAR were the enzymes that showed the best performance under the applied assay conditions. NoCAR had the highest activity towards sodium benzoate compared to NiCAR and NcCAR. Nevertheless, the overall performance of the latter two was also outstanding. For instance, NiCAR and NcCAR were moderately active towards all the hydroxylated substrates, except NcCAR, which showed barely any activity towards protocatechuic acid (PCA) under the assay conditions. Interestingly, NcCAR showed an opposite trend under our applied assay conditions as reported by Schwendenwein and co-workers (2016)¹⁷ who observed that this CAR enzyme was more active towards sodium benzoate and less active towards 4-hydroxybenzoic acid. Other CARs, such as MpCAR, TpCAR and NbCAR also showed some activity towards the selected substrates but they were very low active compared to NoCAR, NiCAR, and NcCAR

CARs were assembled with the *in vitro* recycling system to reduce several carboxylates into their aldehydes. Conversion data are summarized in Table S14.

Table S14. *In vitro* applications of CARs and substrate scope investigation



Conversion ^a (%) of selected carboxylates into their aldehydes				
Enzyme				
<i>No</i> CAR	82±10 >99±0	89±22 >99±0	95±10 >99±0	52±10 93±13
<i>Nb</i> CAR	0 0	0 0	0 0	0 0
<i>Ms</i> CAR	<5 <5	0 0	0 0	0 0
<i>Mp</i> CAR	<5 <5	0 <5	0 9	0 0
<i>Ni</i> CAR	>99 >99	42 >99	41 >99	45 94
<i>Nc</i> CAR	>99 >99	73 >99	64 >99	56 97
<i>Tv</i> CAR	<5 <5	0 0	0 0	0 0
<i>Tp</i> CAR	<5 10	6 16	7 <5	0 13

^aConversion (%) of selected carboxylates into their corresponding aldehyde with integrated *in vitro* cofactor regeneration. No alcohol product was detected in any case. First line refers to the conversion after 1 h of reaction and the second, after 19 h. Reaction conditions: 100 mM MOPS buffer at pH 7.5, 5 mM substrate, 6.25 mM MgCl₂, 100 mM β-D-glucose, 4 mg mL⁻¹ sodium polyphosphate, 0.5 mM NADPH, 1 mM ATP, 100 μg mL⁻¹ purified CAR, 100 μg mL⁻¹ purified *Mr*PPK, 40 μg mL⁻¹ purified *Sm*PPK, 25 μg mL⁻¹ purified *Ec*PPase, 50 μg mL⁻¹ purified GDH, 30 °C, 800 rpm. Reaction volume of 250 μL.

5.2. Conversion curves for 3-hydroxybenzoic acid

NoCAR was assembled with increasing concentrations of 3-OH-BZ (10 and 25 mM) in combination with the *in vitro* setup to regenerate both NADPH and ATP. The conversion curves obtained are presented in Figure S14.

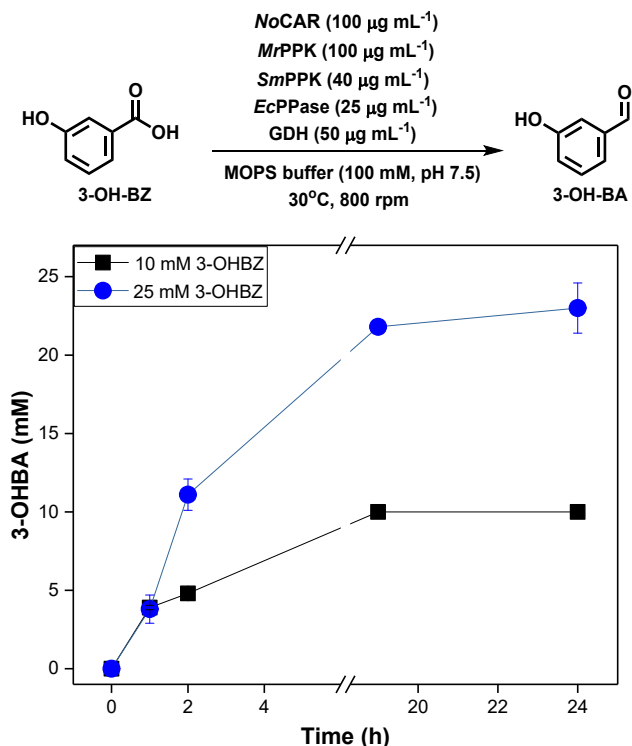


Figure S14. *In vitro* reduction of 3-hydroxybenzoic acid (3-OH-BZ, 10 and 25 mM) using freshly prepared *NoCAR* assembled with an *in vitro* cofactor regeneration system. Reaction conditions: 100 mM MOPS buffer (pH 7.5), 12.5 – 25 mM MgCl₂, 100 mM β-D-glucose, 8 – 25 mg mL⁻¹ sodium polyphosphate, 0.5 mM NADPH, 1 mM ATP, 100 µg mL⁻¹ purified *NoCAR*, 100 µg mL⁻¹ purified *MrPPK*, 40 µg mL⁻¹ purified *SmPPK*, 25 µg mL⁻¹ purified *EcPPase*, 50 µg mL⁻¹ purified GDH, 30 °C, 800 rpm. Data points are the average of three technical replicates. Error bars represent the standard deviation. 3-OH-BA stands for 3-hydroxybenzaldehyde.

According to these data, almost full conversion of 3-OH-BZ into 3-OH-BA was achieved after 18 h of reaction for the reactions starting with 10 mM 3-OH-BZ. Increasing the substrate concentration to 25 mM led to a slower reaction but with very good conversion (>90%) into 3-OH-BA over 24 h reaction. Unfortunately, with concentrations of 3-OH-BZ >25 mM, lower yields were obtained under the tested reaction conditions and we assumed that substrate inhibition could take place (data not shown). Similarly, as in previous results, no overreduction was observed and no 3-OH-benzyl alcohol was detected.

It is important to note that these results were obtained using *NoCAR* that had not been stored for longer than a month. Therefore, reasonably fresh enzyme preparations were used. Fresh formulations of CAR enzymes seem to be ideal since this enzyme can lose activity rapidly depending on the storage method

applied. Therefore, the reproducibility of the results herein presented could be compromised when *NoCAR* stored for a longer periods is used. This is an issue particularly addressed in the main manuscript.

5.3. *In vitro* reduction of 3-hydroxybenzoic acid using long-term stored *NoCAR*

NoCAR preparations (*NoCAR* in Tris-HCl buffer, pH 7, stored as aliquots at -20 °C) stored ≥ 1 month showed reduced catalytic efficiency compared to fresh enzyme preparations. We hypothesized that extra supply of cofactors could be beneficial for the enzyme to give full conversion of the substrate. For this, coenzymes used for the cofactor regeneration (*MrPPK*, *SmPPK*, *EcPPase*) were produced and purified again to guarantee full and efficient performance of the cofactor system. Commercial GDH was also freshly used. Long-term stored *NoCAR* was employed in the reduction of 3-hydroxybenzoic acid using the same reaction conditions as previous experiments, but now with varying concentrations of both cofactors. Besides, the possibility of replacing NADPH by NADH was investigated. Results are shown in Figure S15.

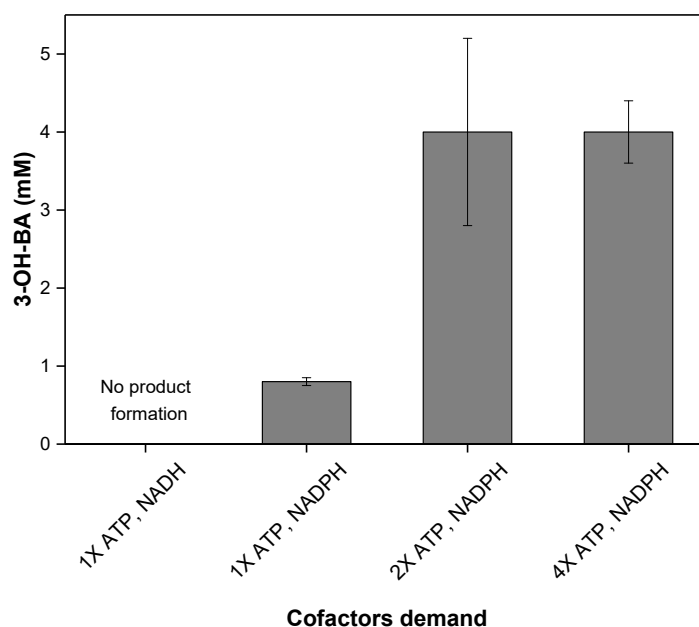


Figure S15. *In vitro* reduction of 3-hydroxybenzoic acid (3-OH-BZ, 10 mM) using a purified *NoCAR* preparation assembled an *in vitro* regeneration of both cofactors. *NoCAR* used in this study had been stored as liquid stock at -20 °C for at least 3 months. Reaction conditions: 100 mM MOPS buffer (pH 7.5), 12.5 mM MgCl₂, 100 mM β -D-glucose, 8 mg mL⁻¹ sodium polyphosphate, 100 μ g mL⁻¹ purified *NoCAR*, 100 μ g mL⁻¹ purified *MrPPK*, 40 μ g mL⁻¹ purified *SmPPK*, 25 μ g mL⁻¹ purified *EcPPase*, 50 μ g mL⁻¹ purified GDH, 30°C, 800 rpm, 3 h of reaction. (1xATP = 1 mM; 1xNAD(P)H = 0.5 mM). Data points are the average of three technical replicates. Error bars represent the standard deviation. 3-OH-BA stands for 3-hydroxybenzaldehyde.

As expected, data shown in Figure S15 show that NADH is not accepted by purified *NoCAR* as hydride donor. In this case, no aldehyde nor alcohol products were detected. When applied *in vitro*, CARs do not

tend to accept any NADH. When employed as whole cell catalysts, cells can replenish depleting NADPH at the cost of NADH to fuel CAR with NADPH. Therefore, replacing NADPH by NADH in *in vitro* NoCAR-catalysed biotransformations was not possible in the applied setup.

As can be also observed in Figure S15, by applying the initial concentration of cofactors (0.5 mM NADPH and 1 mM ATP), about 10% conversion of 3-OH-BZ into 3-OH-BA was observed (1 mM product was formed) after 3 h of reaction. Doubling the concentration of the cofactors led to the formation of about 4 mM 3-OH-BA (about 40% conversion) in the same time span. This represents a 4-fold increase in the product formation compared to the previous applied conditions. However, increasing the concentration of both cofactors even further by 4-fold did not lead to more product formation since the same conversion was obtained (about 4 mM 3-OH-BA, 40% conversion). These results were important to confirm that the amount of cofactors used can strongly affect the reactions catalysed by NoCAR preparations stored for long periods, although the complete recovery of the enzyme activity was still not possible compared to freshly prepared enzyme.

5.4. Determination of the stereoselectivity of the carboligase *ApPDC-var*

To confirm the stereoselectivity of the carboligase, a 2D-UHPLC analysis using a chiral column was used to analyze the product of the carboligation step. Here, standard compounds of each isomer were used to visualize the different retention times due to the nature of the stereocenter. Figure S16 shows an exemplary chromatogram obtained in this analysis.

As can be observed, the product obtained in the carboligation catalysed by *ApPDC-var* is therefore the (*R*)-product. Based on the area under the peaks, the enantiomeric excess (*ee*) was estimated to be >95%.

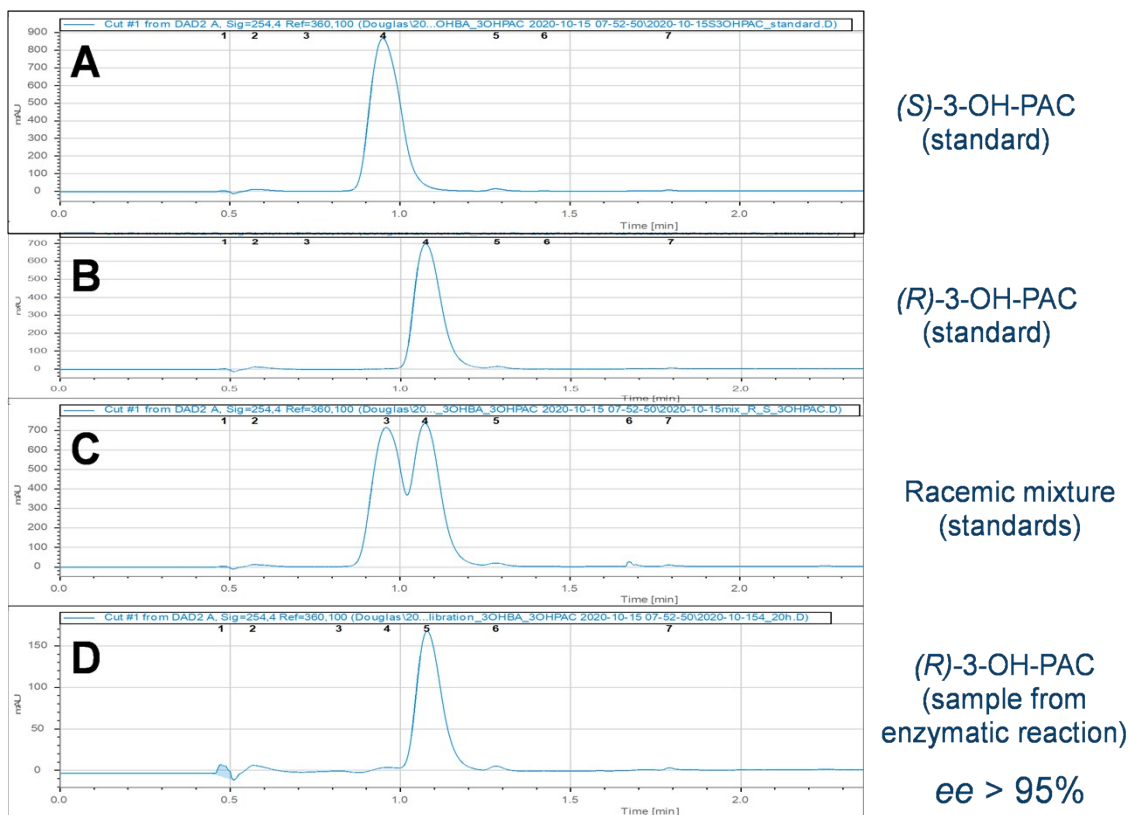
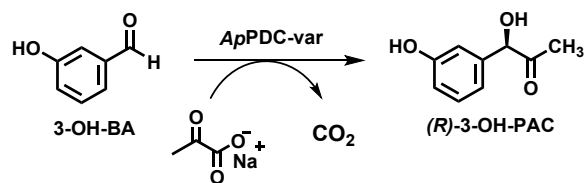
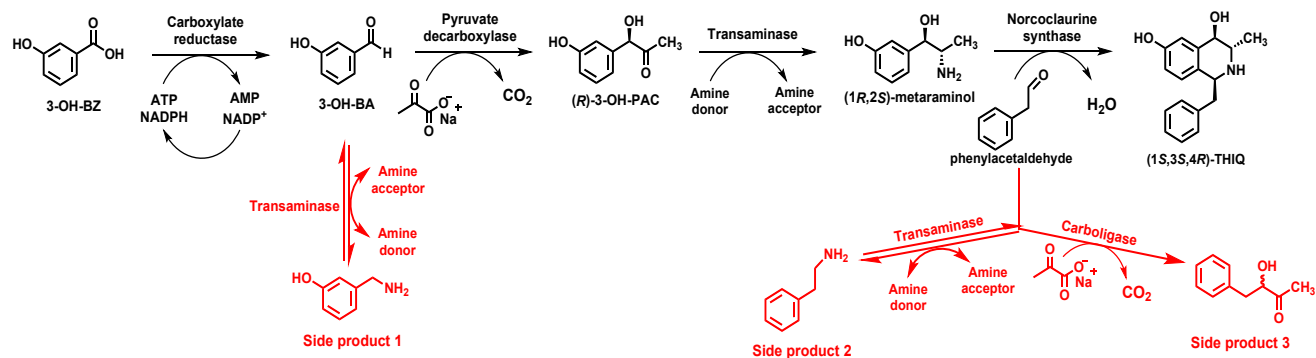


Figure S16. Chromatograms obtained after analysis in a 2D-UHPLC equipped with a chiral column. Peaks show the different positions (retention times) in which the two stereoisomers of 3-OH-PAC are eluted. Standard compounds of each isomer were individually analysed (**A** and **B**), followed by a racemic mixture of them (**C**), and a sample collected from a carbologation reaction catalysed by ApPDC-var (**D**). Reaction conditions of the carbologation: supernatant from previous reaction step containing 9 mM of 3-OH-BA, 100 mM HEPES buffer at pH 6.5, 50 mM sodium pyruvate, 0.1 mM ThDP, 2.5 mM MgSO₄, 2.5% v v⁻¹ DMSO, 0.8 mg protein mL⁻¹ of purified ApPDC-var.

5.5. Cross-reactivity and possible formation of by-products in the cascade

According to Scheme S5, both the carbologase and transaminase show cross-reactivity towards some components of the cascade. The competing routes are shown in red.

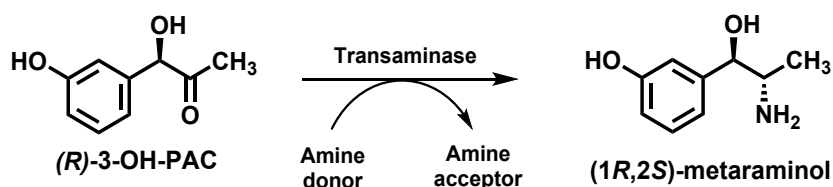


Scheme S5. Four-step cascade towards metaraminol and a substituted THIQ including the possible cross-reactions (in red) due to enzyme promiscuity of both carboligase and transaminase. The formation of side products might occur when the cascade is performed in one-pot system and when no regulation of the enzyme activity is taken into account.

5.6. Optimisation of the transamination reaction

The following reaction parameters were optimised:

- Concentration of *BmTA*
- Molar ratio of substrates
- Reaction mode (opened or closed lid)
- Selection of amine donor



5.6.1. Concentration of *BmTA*

The amount of *BmTA* used in the transamination reaction was one of the first parameters to be evaluated. Therefore, three different concentrations of purified *BmTA* were tested, always based on the protein content determined via Bradford assay. The results obtained are shown in Figure S17.

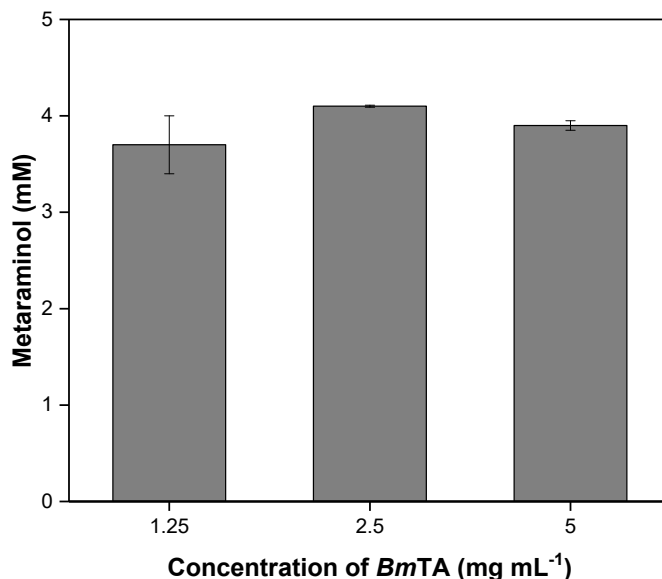


Figure S17. Evaluation of different concentrations of *BmTA* in the transamination of (*R*)-3-OH-PAC with IPA. Reaction conditions: 100 mM HEPES buffer (pH 8), 5 mM (*R*)-3-OH-PAC, 0.3 mM PLP, 10 mM IPA, 1.25 – 5.0 mg protein mL⁻¹ of purified *BmTA*, 3% v v⁻¹ DMSO, 30°C, 2 h, 1000 rpm. Protein content based on Bradford assay. Overall volume = 1 mL. Data points are the average of three technical replicates.

As shown in Figure S17, the three concentrations herein evaluated showed similar outcomes. Reactions performed with 1.25 mg protein mL⁻¹ of *BmTA* yielded in almost 4 mM of (*1R,2S*)-metaraminol (about 80% conversion). Doubling the amount of catalyst, about 4.2 mM of (*1R,2S*)-metaraminol was formed (about 84% conversion). However, using 5 mg protein mL⁻¹ of *BmTA* did not yield more product, totalizing about 4 mM of (*1R,2S*)-metaraminol in the reaction mixture. Thus, the chosen catalyst concentration to conduct further experiments was 2.5 mg protein mL⁻¹ of *BmTA*.

5.6.2. Molar ratio of substrates

Next, the molar ratio of the 2-hydroxy ketone substrate and the amine donor substrate was evaluated. Herein, the ketone substrate is the limiting one and the amine donor is usually used in excess. In the cascade, when starting with 10 mM 3-OH-BZ, the amount of (*R*)-3-OH-PAC in the beginning of the third step is around 5 – 6 mM, considering that high conversions were obtained in the first and second steps as well as the dilutions due to the addition of the other components required in each step. Thus, the amount of amine donor used in this study was calculated starting with 5 mM (*R*)-3-OH-PAC, meaning that a range of 5 – 20 mM amine donor was employed to have a molar ratio series of 1:1, 1:2, and 1:4. The results obtained for the product formation (mM) are shown in Figure S18.

According to the results obtained, the best molar ratio between (*R*)-3-OH-PAC and IPA (amine donor) is 1:4. By using these amounts, about 4.1 mM of (*1R,2S*)-metaraminol, was formed in 2 h of reaction, representing about 80% of substrate conversion. Furthermore, the other two molar ratio evaluated clearly show that the more IPA available the higher is the product yield. However, the maximum amount of IPA accepted by the enzyme (before inactivation) was not investigated. Possibly, higher molar ratios would

be possible, leading to higher product yields. On the other hand, too high concentrations of amine donor in excess are also not economically suitable. Still, it was decided that 1:4 ratio would already offer a sufficient amount of amine donor for the conversion of (*R*)-3-OH-PAC available in the supernatant and still keep the enzyme active.

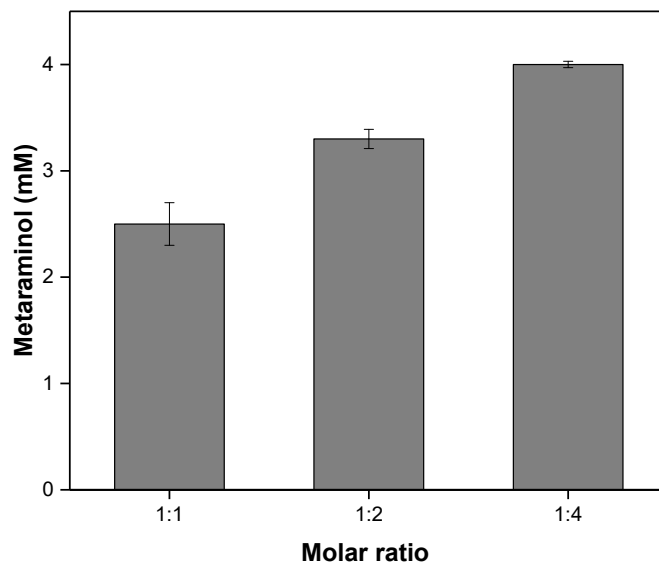


Figure S18. Evaluation of the molar ratio between (*R*)-3-OH-PAC and the amine donor IPA in the transamination reaction catalysed by *BmTA*. Reaction conditions: 100 mM HEPES buffer (pH 8), 5 mM (*R*)-3-OH-PAC, 0.3 mM PLP, 5 – 20 mM IPA, 2.5 mg protein mL⁻¹ of purified *BmTA*, 3% v v⁻¹ DMSO, 30°C, 2 h, 1000 rpm. Overall volume = 1 mL. Data points are the average of three technical replicates.

5.6.3. Reaction mode: closed/opened lid

Subsequently, the influence of leaving the lid of the reaction vial opened or close was investigated. One of the by-products formed in the transamination is acetone (when IPA is the amine donor), which is quite volatile (its boiling point is 56°C) and therefore is easily released out the reaction. According to the Le Chatelier's principle, as soon the concentration of the ketone is released its concentration in the reaction mixture decreases. As a result, the equilibrium is shifted towards the product side to achieve a new equilibrium state. Thus, leaving the lid opened could facilitate the release of the volatile compound and favor the product formation. The results herein obtained are shown in Figure S19.

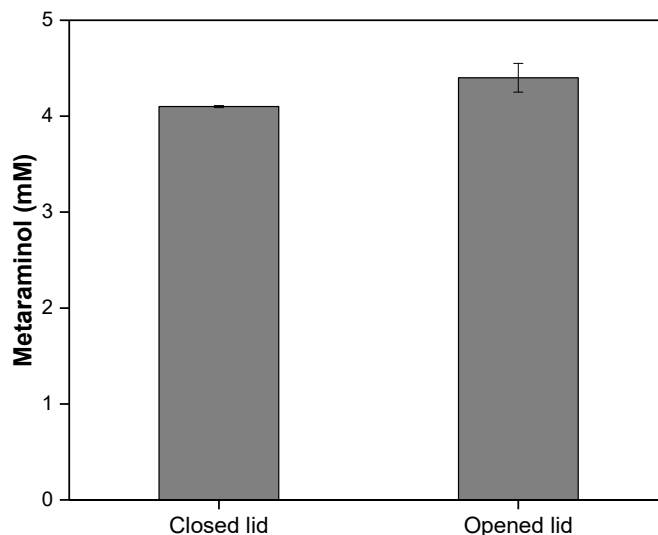


Figure S19. Evaluation of the reaction mode (with or without opened lid) in the transamination of (*R*)-3-OH-PAC with IPA catalyzed by *BmTA*. Reaction conditions: 100 mM HEPES buffer (pH 8), 5 mM (*R*)-3-OH-PAC, 0.3 mM PLP, 10 mM IPA, 2.5 mg protein mL⁻¹ of purified *BmTA*, 3% v v⁻¹ DMSO, 30°C, 2 h, 1000 rpm. Overall volume = 1 mL. Data points are the average of three technical replicates.

According to the data shown in Figure S19, no major difference was observed leaving the reaction with opened or closed lid. When the lid was opened, a slightly higher amount of product was formed when compared to the reaction with closed lid (4.4 and 4.1 mM, of (1*R*,2*S*)-metaraminol, respectively). For low concentrations of substrate (as in this case), the influence of opened/closed lid is probably very subtle. This factor would probably have a more pronounced effect when scaling-up this reaction to higher substrate concentrations. Still, it was interesting to see that this parameter might be relevant at some point. For now, we opted to leave the reaction vial opened when performing the transamination step to guarantee full performance towards the formation of (1*R*,2*S*)-metaraminol.

5.6.4. Selection of enzyme and amine donor

Up to this point, all experiments targeting to find the optimal reaction conditions for the transamination were performed with *BmTA* as catalyst. The main reason for this choice is that this TA is faster than the one previously used, *Cv2025*. After some optimisation rounds, the best conditions were applied and exploited to reactions catalysed by *Cv2025*. The goal of this experiment was to compare both enzymes in terms of their efficiency in producing (1*R*,2*S*)-metaraminol under the optimal reaction conditions identified for *BmTA*. In addition, the amine donors IPA and α -MBA were compared to check which one would be the most beneficial one with respect to enzyme tolerance and equilibrium shift. The results are shown in Figure S20.

According to the data shown in Figure S20, one of the first observations is that *BmTA* performed better than *Cv2025*, independently on the amine donor used. In 2 h of reaction, *BmTA* was able to produce approximately 2.1 mM and 1.5 mM (1*R*,2*S*)-metaraminol when IPA and α -MBA served as amine donors,

respectively. On the other hand, Cv2025 could produce about 1.4 mM and >1 mM (1*R*,2*S*)-metaraminol in the same period when IPA and α -MBA served as amine donors, respectively. These findings show that:

- *BmTA* had a superior performance and therefore it should be the preferred TA to be applied in the cascade.
- IPA served as a better amine donor, under applied reaction conditions, compared to α -MBA; therefore, the cheaper amine donor (IPA) was chosen for future experiments.

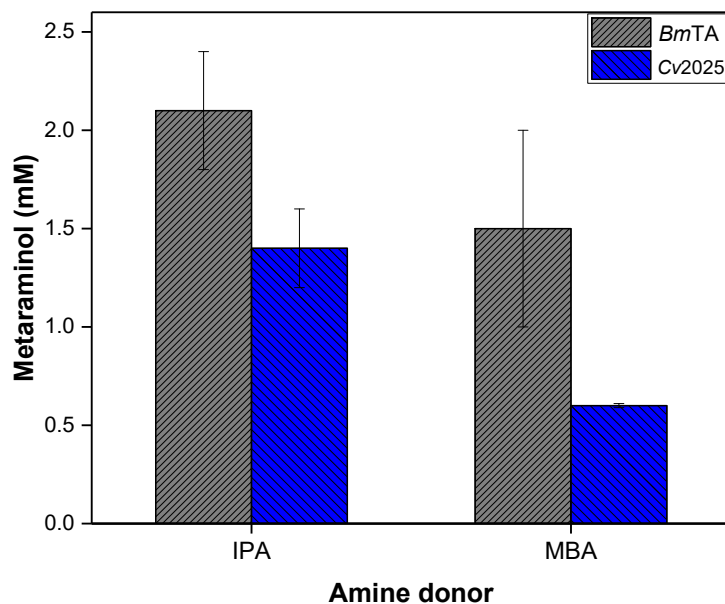


Figure S20. Comparing the performance of *BmTA* and Cv2025 on accepting IPA or α -MBA as amine donors in the transamination reaction to produce (1*R*,2*S*)-metaraminol. Reaction conditions: 100 mM HEPES buffer (pH 8), 5 mM (*R*)-3-OH-PAC, 0.3 mM PLP, 10 mM amine donor, 2.5 mg protein mL⁻¹ of purified *BmTA* or Cv2025, 3% v/v DMSO, 30°C, 2 h, 1000 rpm. Overall volume = 1 mL. Protein content based on Bradford assay. Data points are the average of three technical replicates.

5.6.5. Application of best reaction conditions in the cascade

With this in mind, two cascades starting with 3-OH-BZ were performed in parallel until the formation of (*R*)-3-OH-PAC (obtained with product yields of 96%). Subsequently, the supernatants of the second step were used as substrate for the amine transaminase reaction. Here, *BmTA* and Cv2025 were employed as catalysts in the presence of IPA. Under optimal reaction conditions, reactions were carried out for longer periods and the formation of (1*R*,2*S*)-metaraminol was monitored over time. The product formation in terms of HPLC yield was determined and is shown in Figure S21.

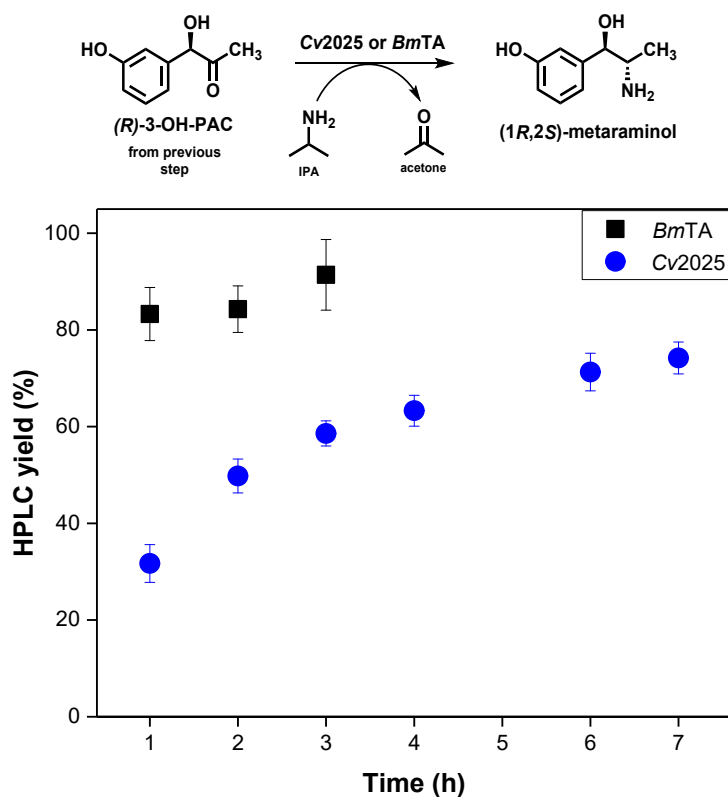


Figure S21. Comparing the performance of *BmTA* and *Cv2025* applying optimal reaction conditions in the transamination of (*R*)-3-OH-PAC with IPA to produce (1*R*,2*S*)-metaraminol. Reaction conditions: 100 mM HEPES buffer (pH 8), 5 mM (*R*)-3-OH-PAC, 0.3 mM PLP, 20 mM amine donor, 2.5 mg protein mL⁻¹ of purified *BmTA* or *Cv2025*, opened lid, 30°C, 1000 rpm. Overall volume = 1 mL. Data points are the average of three technical replicates.

As the data show, reactions catalysed by *BmTA* achieved almost full conversion of (*R*)-3-OH-PAC into (1*R*,2*S*)-metaraminol in 3 h (91 ± 7% HPLC yield). Unfortunately, several experiments performed longer than 3 h showed reduced formation of the product, probably due to some shift in the equilibrium. Therefore, 3 h of for the *BmTA*-catalyzed reaction was set as ideal reaction time.

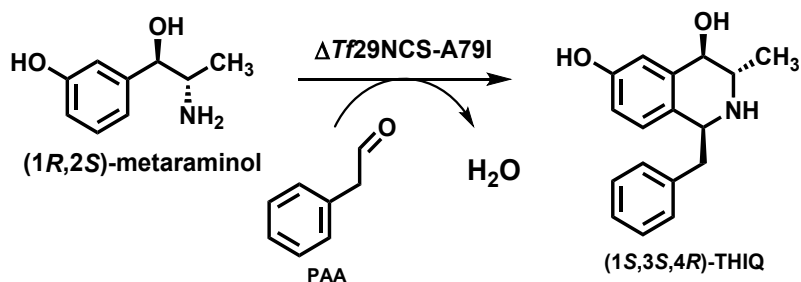
Though *Cv2025* had a great performance, achieving about 74 ± 3% product yield after 7 h reaction, *BmTA* outperformed it and in a reduced time of reaction. Erdmann and co-workers¹³ reported product yields of 93% in 8 h of reaction using *Cv2025* in a similar cascade towards the same product. Most likely, *Cv2025* could achieve similar results obtained with *BmTA* if leaving the reaction longer. Still, for our purposes *BmTA* and IPA proved to be the best amine transaminase and amine donor, respectively, to be applied in the targeted cascade.

5.7. Optimisation of the cyclisation reaction

The following reaction parameters were optimised:

- Concentration of Δ297fNCS-A79I
- Molar ratio of substrates

- Concentration of co-solvent



5.7.1. Concentration of $\Delta 297fNCS-A79I$

The first parameter to be evaluated was the concentration of enzyme. The different concentrations (0.5 – 2.0 mg protein mL⁻¹) were evaluated and the production of (1*S*,3*S*,4*R*)-THIQ was determined by HPLC analytics. The results obtained after 2 h of reaction time are shown in Figure S22.

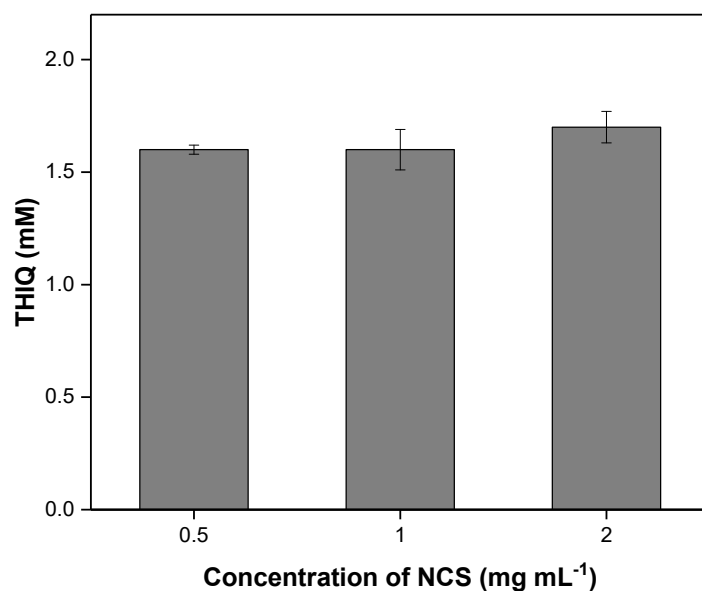


Figure S22. Evaluation of different concentrations of $\Delta 297fNCS-A79I$ in the cyclisation reaction between (1*R*,2*S*)-metaraminol with phenylacetaldehyde (PAA). Reaction conditions: 100 mM HEPES buffer (pH 7.5), 5 mM (1*R*,2*S*)-metaraminol, 5 mM PAA, 0.5 – 2.0 mg protein mL⁻¹ of purified $\Delta 297fNCS-A79I$, 15% v v⁻¹ DMSO, 37°C, 2 h, 850 rpm. Overall volume = 1 mL. Data points are the average of three technical replicates.

According to Figure S22, no difference was observed in the production of (1*S*,3*S*,4*R*)-THIQ with increasing concentration of biocatalyst. Using 0.5 or 1.0 mg protein mL⁻¹ of purified $\Delta 297fNCS-A79I$ yielded the same amount of product (1.6 mM). Increasing the concentration of enzyme up to 2.0 mg protein mL⁻¹ yielded 1.7 mM of (1*S*,3*S*,4*R*)-THIQ. The concentration of 1.0 mg protein mL⁻¹ of $\Delta 297fNCS-A79I$ was selected as preferred one for further experiments. Although this amount did not yield more product compared to the lowest concentration of enzyme tested, we wanted to make sure that the reaction would not be limited

by the catalyst amount. In addition, the reaction in this study was conducted only for 2 h and no full conversion was achieved in any of the reaction performed; therefore, probably longer reaction times would be necessary and a slightly higher concentration of enzyme ($> 0.5 \text{ mg protein mL}^{-1}$) should be added to guarantee maximal product formation.

5.7.2. Substrate molar ratio

Subsequently, the substrate molar ratio was investigated. (1*R*,2*S*)-Metaraminol is the limiting reagent and therefore the concentration of PAA was increased to obtain the following molar ratios: 1:1, 1:2, and 1:4. The formation of (1*S*,3*S*,4*R*)-THIQ was determined after 2 h of reaction and the results are shown in Figure S23.

As shown, the higher the substrate molar ratio the higher was the product formation. For instance, using equimolar concentrations of the substrates yielded less than 2 mM (1*S*,3*S*,4*R*)-THIQ (>40% conversion). Doubling the concentration of PAA enhanced the product concentration almost 1.7-fold in the same period of time (3.4 mM (1*S*,3*S*,4*R*)-THIQ, 68% conversion). Increasing the substrate molar ratio up to 1:4 was sufficient to fully convert the substrate into (1*S*,3*S*,4*R*)-THIQ in 2 h of reaction. Clearly, the molar ratio was the parameter that most affected the product formation in the cyclisation reaction, compared to the previous parameters evaluated. Thus, the molar ratio of 1:4 between metaraminol and PAA was selected for further experiments.

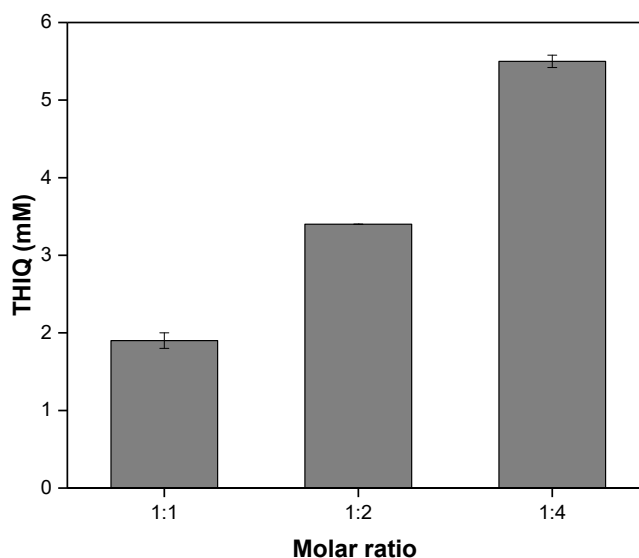


Figure S23. Evaluation of the molar ratio between (1*R*,2*S*)-metaraminol and PAA in the cyclisation reaction catalysed by $\Delta 297fNCS-A79I$. Reaction conditions: 100 mM HEPES buffer (pH 7.5), 5 mM (1*R*,2*S*)-metaraminol, 5 mM PAA, 1.0 mg protein mL^{-1} of purified $\Delta 297fNCS-A79I$, 15% v/v DMSO, 37°C, 2 h, 850 rpm. Overall volume = 1 mL. Data points are the average of three technical replicates.

5.7.3. Concentration of DMSO

The last reaction parameter evaluated in this set of optimization experiments was the concentration of DMSO. Here, DMSO is required to avoid the formation of a second phase, as PAA is poorly soluble in water. Therefore, stock solutions of PAA were prepared in 100% DMSO and then a determined volume of this stock was transferred to the buffer system. In this approach, a final DMSO content of 5% v v⁻¹ was obtained; therefore, this was the minimum amount of this co-solvent that was used. We evaluated whether extra addition of DMSO (up to 15% v v⁻¹) would enhance the product yield by enhancing the solubility of PAA when added to the buffer system. The product formation was determined after 2 h of reaction and the results obtained is shown in Figure S24.

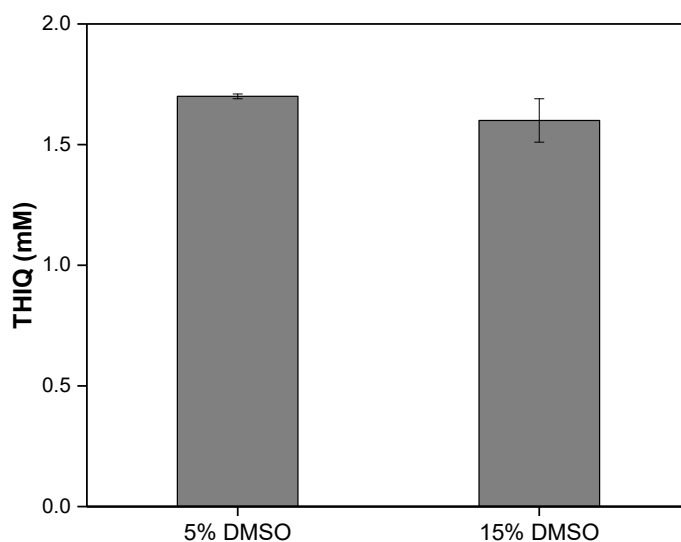


Figure S24. Evaluation of different concentrations of the co-solvent DMSO in the cyclisation reaction of (1*R*,2*S*)-metaraminol and PAA catalysed by $\Delta 297f$ NCS-A79I. Reaction conditions: 100 mM HEPES buffer (pH 7.5), 5 mM (1*R*,2*S*)-metaraminol, 5 mM PAA, 1.0 mg protein mL⁻¹ of purified $\Delta 297f$ NCS-A79I, 5 or 15% v v⁻¹ DMSO, 37°C, 2 h, 850 rpm. Overall volume = 1 mL. Data points are the average of three technical replicates.

As can be observed in Figure S24, a slightly higher concentration of (1*S*,3*S*,4*R*)-THIQ was formed when 5% DMSO was present in the reaction mixture (1.7 mM) compared to when 15% DMSO was used. Increasing the concentration of DMSO to 15% v v⁻¹ yielded about 1.6 mM (1*S*,3*S*,4*R*)-THIQ. With these observations, it is possible to conclude that keeping the concentration of DMSO the lowest possible might be beneficial for the enzyme. In this case, DMSO enhanced the solubility of the co-substrate PAA but probably could affect the stability of the enzyme when used in high concentration. Therefore, the concentration of DMSO of 5% v v⁻¹ was fixed for further experiments. Nevertheless, for scaling-up and subsequent work-up of the reaction it has to be evaluated again if addition of DMSO is advantageous as it clearly challenges downstream process.

5.8. Influence of varying amounts of CAR as lyophilised whole-cell catalysts in the reduction of 3-hydroxybenzoic acid

Increasing amounts of lyophilised *E. coli* K-12 MG1655 cells expressing *NoCAR* and *EcPPTase* were used to reduce 3-OH-BZ. The product formation (3-OH-BA) was determined and the results are presented in Figure S25.

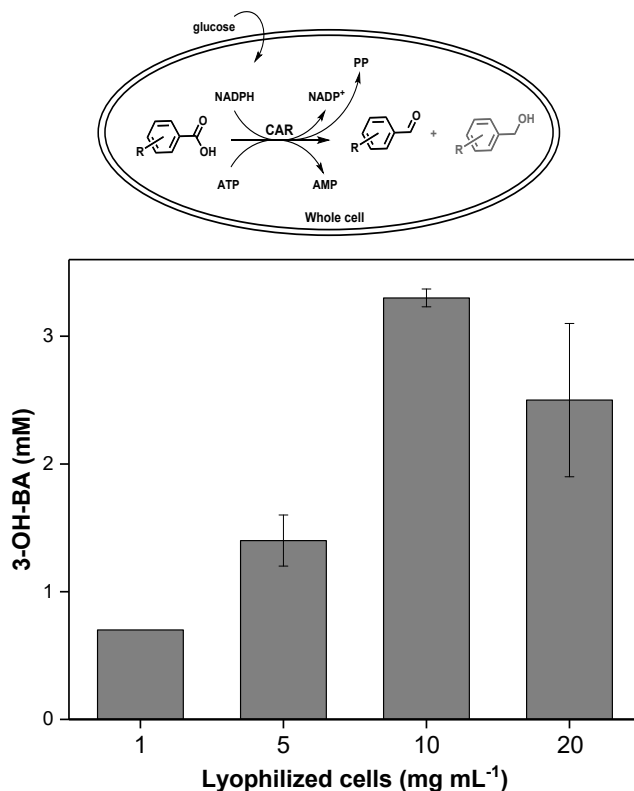


Figure S25. Product formation of the bioreduction of 3-hydroxybenzoic acid (3-OH-BZ, 10 mM) using increasing amounts of *E. coli* K-12 MG1655 (RARE) lyophilised cells co-expressing *NoCAR* and *EcPPTase*. Reaction conditions: 200 mM MOPS buffer (pH 7.5), 25 mM MgCl₂, 48 mM β-D-glucose, 24 mM sodium citrate, 0.5 mM NADPH, 1 mM ATP, 1 – 20 mg mL⁻¹ lyophilized cells expressing *NoCAR*, 30°C, 1000 rpm, 2 h reaction. Reaction volume of 1 mL. Reactions were performed in technical triplicates. Error bars represent the standard deviation. Abbreviation: 3-OH-BA: 3-hydroxybenzaldehyde.

According to Figure S25, the optimal amount of cells is 10 mg mL⁻¹, in which 3.3 mM of 3-OH-BA was formed after 2 h of reaction. Doubling the concentration of biocatalyst did not enhance the product yields (2.5 mM 3-OH-BA); therefore, 10 mg mL⁻¹ was the concentration chosen for further experiments using CARs as whole-cell catalysts. It is important to mention that no alcohol was formed in any of the reactions performed, probably because the reactions were carried out only for 2 h. Leaving the reaction longer, aiming full conversion of the substrate, would probably lead to some alcohol formation, as observed in Figure 4 in the main manuscript.

5.9. Increasing substrate loads in the bioreduction of 3-hydroxybenzoic acid catalysed by whole-cell catalysts

Increasing concentrations of 3-OH-BZ were tested with lyophilised *E. coli* K-12 MG1655 (RARE) cells co-expressing *NoCAR* and *EcPPTase*. The results are shown in Figure S26.

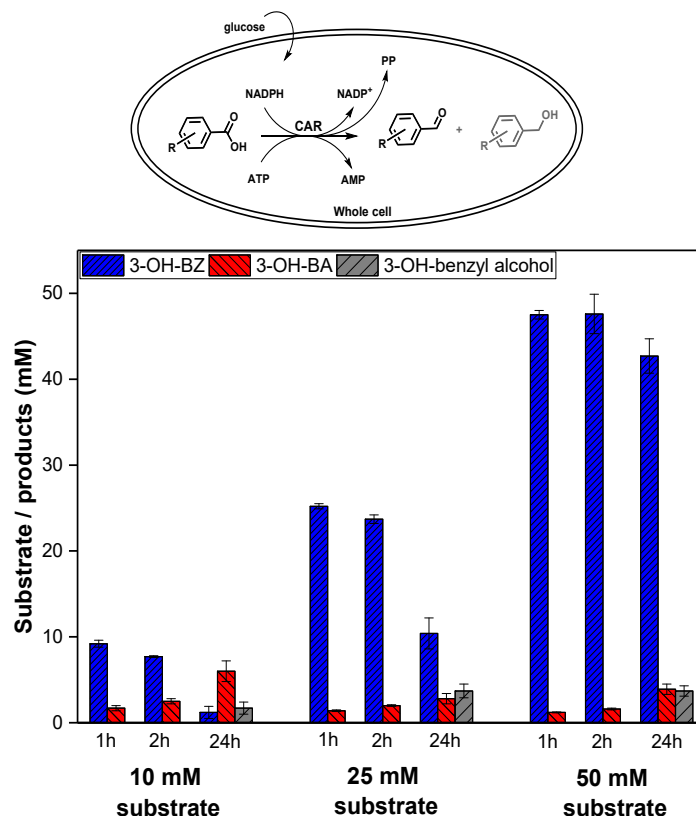


Figure S26. Reduction of increasing loads of 3-hydroxybenzoic acid (3-OH-BZ, 10 – 50 mM) using lyophilised *E. coli* K-12 MG1655 (RARE) cells co-expressing *NoCAR* and *EcPPTase*. Reaction conditions: 200 mM MOPS buffer (pH 7.5), 25 mM MgCl₂, 48 mM β-D-glucose, 24 mM sodium citrate, 0.5 mM NADPH, 1 mM ATP, 10 mg mL⁻¹ lyophilized cells expressing *NoCAR* and *EcPPTase*, 30°C, 1000 rpm. Reaction volume of 1 mL. Reactions were performed in technical triplicates. Error bars represent the standard deviation. Abbreviations: 3-OH-BA: 3-hydroxybenzaldehyde; 3-OH-benzyl alcohol: 3-hydroxybenzyl alcohol.

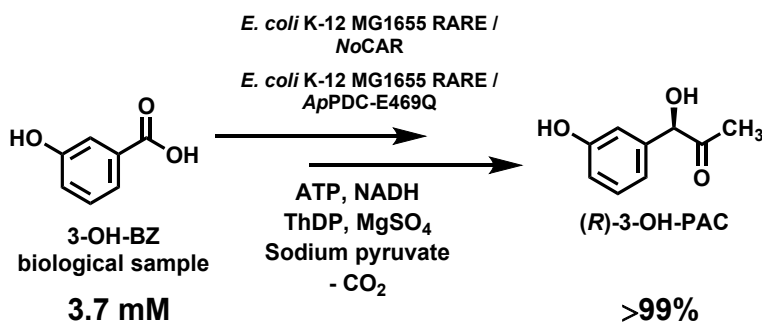
According to these data, bioreductions starting with substrate concentration higher than 10 mM did not perform well. When 10 mM 3-OH-BZ was used, about 72% of the substrate was consumed in 24 h, producing approximately 6 mM of 3-OH-BA and 1.2 mM of the alcohol. Increasing the concentration of 3-OH-BZ to 25 mM, less than 3 mM of 3-OH-BA were formed after 24 h of reaction and about 4 mM of the alcohol were present in the reaction mixture.

Results were even worse for the bioreductions starting with 50 mM 3-OH BZ. In this case, only 8% of the substrate was converted into a 50% mixture of the aldehyde and the alcohol (about 4 mM of each one

was formed). Bioreductions starting with 75 and 100 mM 3-OH-BZ were also performed, but the outcome was similarly unfavorable (data not shown). Thus, it became clear that either substrate inhibition could be happening, or the cofactor regeneration was not sufficient (or a combination of both facts). Therefore, performing the reduction of 3-OH-BZ as single-step reaction was not the ideal mode.

5.10. Proof-of-concept one-pot two-step cascade starting with renewable 3-OH-BZ

According to the data shown in Scheme 2 of the main manuscript, the commercially available 3-OH-BZ could be efficiently applied as substrate in both biocatalytic cascade approaches. As stated previously, one of our goals was to apply substrates gained from renewable resources in the cascades towards more complex molecules. Microbial cell factories using *Corynebacterium glutamicum* as platform for the production of several hydroxybenzoates (including 3-OH-BZ)¹⁸ were developed by cooperation partners and the fermentation broths containing 3-OH-BZ as main product were kindly donated to us. One of the limitations faced here was the low titers (about 3.7 mM) of the fermentation broths containing 3-OH-BZ, limiting further applications in the four-step cascade towards (1*S*,3*S*,4*R*)-THIQ. Therefore, we decided to explore the applicability of this renewable substrate only in a two-step one-pot cascade to obtain (*R*)-3-OH-PAC ((*R*)-**3** in Scheme 1 of the main manuscript), which is already a target substance for industrial processes as being a building block for other classes of compounds. The overall cascade is shown in Scheme S6.



Scheme S6. Two-step one pot cascade towards (*R*)-3-OH-PAC starting with microbially produced 3-OH-BZ using lyophilised whole-cell catalysts. Reaction conditions: 200 mM MOPS buffer (pH 7.5), filtered supernatant of a fermentation broth containing 3.7 mM 3-OH-BZ, 5-fold sodium pyruvate, 4 mM MgSO₄, 48 mM glucose, 24 mM sodium citrate, 1 mM ThDP, 1 mM ATP, 0.5 mM NADH, 10 mg mL⁻¹ lyophilised *E. coli* K-12 MG1655 RARE cells expressing *NoCAR* and *EcPPTase*, 10 mg mL⁻¹ lyophilised *E. coli* K-12 MG1655 RARE cells expressing *ApPDC-var*, 30°C, 850 rpm, 20 h.

The two-step cascade using lyophilised whole-cell catalysts (as shown in Figure 5A of the main manuscript) was chosen over the *in vitro* biocatalytic process due to (i) the outstanding results obtained using whole-cells catalysts (ii) the possibility to avoid further dilution of the supernatant containing 3-OH-BZ

(performing a sequential cascade would demand more dilution of the supernatant containing the substrate). By applying the conditions described in the Experimental section of in the main manuscript, full conversion of the substrate was achieved and >99% HPLC yield was obtained after 20 h of reaction. Although the fermentation broth contained mainly 3-OH-BZ, several other compounds from the fermentation were still present, including tiny amount of the other hydroxybenzoates and the alcohol side products. Nevertheless, the presence of these additional substances seemed not to interfere in the formation of (*R*)-3-OH-PAC. Another reason that could explain the high product yields obtained in this proof-of-concept was the fact that 3-OH-BZ was present in a considerable low concentration and therefore its total conversion could have been achieved faster compared to the reactions starting with chemically produced 3-OH-BZ. Overall, these results are promising to confirm the applicability of crude fermentation broths containing the desired substrate directly in enzymatic cascades targeting more complex molecules, such as (*R*)-3-OH-PAC. Other compounds in the broth seem not to hamper the catalyst performance too negatively.

Overall, this two-step cascade starting with renewable 3-OH-BZ is a great example of a hybrid process that could fill the gap between aromatic carboxylic acids obtained from microbial cell factories and enzyme cascades targeting important pharmaceutical precursors.

6. References

- 1 J. Taylor-Parker, Plasmids 101: *E. coli* Strains for Protein Expression, Available at <https://blog.addgene.org/plasmids-101-e-coli-strains-for-protein-expression>, (Accessed 16 July 2021).
- 2 Novagen Catalog User Protocol, *Competent Cells Overview*, 2003, 1-23. Available at <http://wolfson.huji.ac.il/expression/procedures/bacterial/novagen-CompCells.pdf> - accessed on 20.03.23.
- 3 A. M. Kunjapur, Y. Tarasova and K. L. J. J. Prather, *J Am Chem Soc*, 2014, **136**, 11644–11654.
- 4 W. Finnigan, A. Thomas, H. Cromar, B. Gough, R. Snajdrova, J. P. Adams, J. A. Littlechild and N. J. Harmer, *ChemCatChem*, 2017, **9**, 1005–1017.
- 5 M. Moura, D. Pertusi, S. Lenzini, N. Bhan, L. J. Broadbelt and K. E. J. Tyo, *Biotechnol Bioeng*, 2016, **113**, 944–952.
- 6 H. Stolterfoht, D. Schwendenwein, C. W. Sensen, F. Rudroff and M. Winkler, *J Biotechnol*, 2017, **257**, 222–232.
- 7 D. Weber, D. Patsch, A. Neumann, M. Winkler and D. Rother, *ChemBioChem*, 2021, **22**, 1823–1832.
- 8 M. Winkler and C. K. Winkler, *Monatsh Chem*, 2016, **147**, 575–578.
- 9 A. E. Parnell, S. Mordhorst, F. Kemper, M. Giurrandino, J. P. Prince, N. J. Schwarzer, A. Hofer, D. Wohlwend, H. J. Jessen, S. Gerhardt, O. Einsle, P. C. F. Oyston, J. N. Andexer and P. L. Roach, *Proc Natl Acad Sci U S A*, 2018, **115**, 3350–3355.
- 10 S. Mordhorst, J. Siegrist, M. Müller, M. Richter and J. N. Andexer, *Angew Chem Int Edit*, 2017, **56**, 4037–4041.
- 11 M. Pfeiffer, D. Bulfon, H. Weber and B. Nidetzky, *Adv Synth Catal*, 2016, **358**, 3809–3816.

- 12 G. A. Strohmeier, I. C. Eiteljörg, A. Schwarz and M. Winkler, *Chem-Eur J.*, 2019, **25**, 6119–6123.
- 13 V. Erdmann, B. R. Lichman, J. Zhao, R. C. Simon, W. Kroutil, J. M. Ward, H. C. Hailes and D. Rother, *Angew Chem Int Edit*, 2017, **56**, 12503–12507.
- 14 T. Sehl, S. Bock, L. Marx, Z. Maugeri, L. Walter, R. Westphal, C. Vogel, U. Menyes, M. Erhardt, M. Müller, M. Pohl and D. Rother, *Green Chem*, 2017, **19**, 380.
- 15 T. Sehl, H. C. Hailes, J. M. Ward, U. Menyes, M. Pohl and D. Rother, 2014, **16**, 3341.
- 16 J. Wachtmeister, A. Jakoblinnert and D. Rother, *Org Process Res Dev*, 2016, **20**, 1744–1753.
- 17 D. Schwendenwein, G. Fiume, H. Weber, F. Rudroff and M. Winkler, *Adv Synth Catal*, 2016, **358**, 3414–3421.
- 18 N. Kallscheuer and J. Marienhagen, *Microb Cell Fact*, 2018, **17**, 1–13.